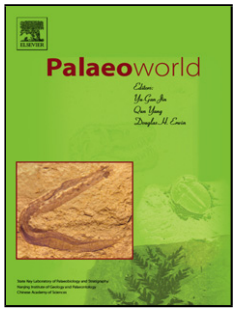

Title: Correlating the global Cambrian–Ordovician boundary: precise comparison of the Xiaoyangqiao section, Dayangcha, North China with the Green Point GSSP section, Newfoundland, Canada

Authors: Xiao-Feng Wang, Svend Stouge, Jörg Maletz, Gabriella Bagnoli, Yu-Ping Qi, Elena G. Raevskaya, Chuan-Shang Wang, Chun-Bo Yan

PII: S1871-174X(18)30110-0
DOI: https://doi.org/10.1016/j.palwor.2019.01.003
Reference: PALWOR 488

To appear in: *Palaeoworld*

Received date: 14 July 2018
Revised date: 29 November 2018
Accepted date: 22 January 2019

Please cite this article as: Wang, Xiao-Feng, Stouge, Svend, Maletz, Jörg, Bagnoli, Gabriella, Qi, Yu-Ping, Raevskaya, Elena G., Wang, Chuan-Shang, Yan, Chun-Bo, Correlating the global Cambrian–Ordovician boundary: precise comparison of the Xiaoyangqiao section, Dayangcha, North China with the Green Point GSSP section, Newfoundland, Canada.Palaeoworld https://doi.org/10.1016/j.palwor.2019.01.003

Correlating the global Cambrian–Ordovician boundary: precise comparison of the Xiaoyangqiao section, Dayangcha, North China with the Green Point GSSP section, Newfoundland, Canada

Xiao-Feng Wang[a], Svend Stouge[b,*], Jörg Maletz[c], Gabriella Bagnoli[d], Yu-Ping Qi[e,f], Elena G.Raevskaya[g], Chuan-Shang Wang[a], Chun-Bo Yan[a]

[a]Wuhan Center of China Geological Survey (Wuhan Institute of Geology and Mineral Resources), Wuhan, China; *E-mail addresses*: ycwangxiaofeng@163.com, wangchuanshang@163.com, yanchunbo123@163.com

[b]Natural History Museum of Denmark, University of Copenhagen, Copenhagen, Denmark; *E-mail address*: svends@snm.ku.dk

[c]Institute of Geology, Free University of Berlin, Germany; *E-mail address*: yorge@zedat.fu-berlin.de

[d]Dipartimento di Scienze della Terra, Via S. Maria 53, I-56126 Pisa, Italy; *E-mail address*: gabriella.bagnoli@unipi.it

[e]State Key Laboratory of Palaeobiology and Stratigraphy, Nanjing Institute of Geology and Palaeontology, Chinese Academy of Sciences, 39 East Beijing Road, Nanjing 210008, China; *E-mail address*: ypqi@nigpas.ac.cn

[f]Center for Excellence in Life and Palaeoenvironment, Nanjing Institute of Geology and Palaeontology, Chinese Academy of Sciences, 39 East Beijing Road, Nanjing 210008, China

[g]AO 'Geologorazvedka', Fayansovaya Street 20, Building 2A, Saint Petersburg 191019, Russia; *E-mail address*: lena.raevskaya@mail.ru

[*]Corresponding author.

Abstract

The Cambrian–Ordovician boundary interval exposed at the Xiaoyangqiao section, North China is presented. The distribution of stratigraphically important fossils in the Xiaoyangqiao section revealed several nearly coeval graptolite, conodont, trilobite, and acritarch bioevents in the uppermost Cambrian–lowermost Ordovician carbonate-siliciclastic sedimentary sequence. The precise correlation to the Green Point GSSP section, western Newfoundland, Canada allows for the identification of the corresponding GSSP level in the Xiaoyangqiao section. The combined data from the Xiaoyangqiao section and the Green Point GSSP section

provide a series of events that all can be applied as proxies for identification of the Cambrian–Ordovician boundary horizon outside the GSSP. Based on this, the Xiaoyangqiao section, Dayangcha, is here strongly recommended as a candidate for an Auxiliary Boundary Stratigraphic Section and Point section (ASSP) for the base of the Ordovician System, because it provides one of the best and most complete Cambrian–Ordovician transitions in the world and because the first planktonic graptolites are from the Xiaoyangqiao section.

Keywords: Dayangcha ASSP section; Green Point GSSP section; Cambrian–Ordovician boundary; acritarchs; conodonts; graptolites

1. Introduction

Recognition of the boundary between the Cambrian and Ordovician systems is a matter of global scale discussions. During the last couple of decades, several integrated studies of Cambrian–Ordovician boundary sections from different regions were published with the objective to show the presence of the chosen biological marker in these sections and the potential for correlation of the Cambrian–Ordovician boundary (e.g., Albanesi et al., 2015; Zhen et al., 2017). The latest Cambrian to Early Ordovician transition (ca. 485.4 Ma; based on the International Chronostratigraphic Chart 2017/2), representing an important episode in Earth History, is excellently displayed in the Xiaoyangqiao section (= lower part of the Xiaoyangqiao composite section (XCS) of Chen et al. (1985, 1986, 1988)), Dayangcha, North China. In comparison with coeval successions from Europe and Asia, the stratigraphically continuous Cambrian–Ordovician limestone-shale succession at the Xiaoyangqiao section offers one of the best possibilities to document the Cambrian–Ordovician transition over a wide area and on a global scale. The Xiaoyangqiao section, close to the township Dayangcha (Fig. 1), is here recommended as a global Auxiliary Boundary Stratigraphic Section and Point (ASSP) because it comprises a complete conodont, graptolite, acritarch and trilobite succession; moreover, the $\delta^{13}C_{carb}$ isotope data, the sequence stratigraphy, and magnetostratigraphy provide additional and important results, enabling precise comparison with known key and widely separated sections and the Cambrian–Ordovician boundary in the world.

This paper discusses the results of the new integrated study using two macrofossil groups (graptolites, trilobites) and two microfossil groups, i.e., conodonts and acritarchs, as well as stable isotope data ($\delta^{13}C_{carb}$, $\delta^{18}O$), sea-level changes and sequence stratigraphy in the

Xiaoyangqiao section and the comparison with the Green Point GSSP section in Newfoundland, Canada.

1.1. The Cambrian–Ordovician line: a historical review

The International Working Group on the Cambrian–Ordovician Boundary (COBWG I) was established in 1974. In this period, members of the Working Group visited several proposed candidate boundary sections, which were widely distributed in the world (Australia, China, Great Britain, Kazakhstan, North America and Scandinavia). The Working Group arranged many workshops, field meetings and conferences that all were devoted towards the Cambrian–Ordovician boundary. The working group documented these activities, discussions and the decisions/results in numerous reports and publications (e.g., Norford, 1991).

The extensive list of publications includes the volumes of papers on candidate boundary sections published in Bassett and Dean (1982) and Norford and Webby (1988). Chen et al. (1985) and Chen (1986) published two special volumes of papers, specifically on the Dayangcha section, covering a wide range of disciplines. Additional papers concerning issues on the Cambrian–Ordovician boundary appeared in Barnes and Williams (1991) and Webby and Laurie (1992).

The first working group also discussed the principles, procedures, candidate sections, and discussed the boundary definition, and various potential levels for the boundary. One main activity of the Working Group was the selection of the level for the boundary and subsequently, the choice of the marker taxon became important. After 19 years and replacement of three chairmens, this first working group and the executive and voting members stepped down in 1993. The second working group (GOBWG II) was established in 1993. In this period, the members visited and investigated in detail the Dayangcha, Green Point, and Lawson Cove candidate sections.

At the working meeting held in Canada in 1985 the COBWG I proposed that the Cambrian–Ordovician boundary should be drawn at the level below but close to the appearance of first planktic graptolites and marked by the FAD (First Appearance Datum) of a species of the complete evolutionary succession of the conodont genus *Cordylodus* Pander (Barnes, 1988; Nicoll, 1990, 1992).

However, due to systematic problems with the originally proposed conodont marker *Cordylodus lindstromi* (i.e., Barnes, 1988) this taxon was abandoned and instead the conodont species *Iapetognathus fluctivagus* Nicoll et al., 1999 was introduced as the primary marker for the Cambrian–Ordovician boundary (Nicoll et al., 1999). Accordingly, the Green Point

section, Newfoundland, Canada, became the only candidate for the GSSP section for the base of the Ordovician System, because both the marker species and planktic graptolites are present in the section.

Succeeding the selection of Green Point as the GSSP section several problems remained and new ones arose. One of the remaining problems is the difficulty in correlating shallow-water deposits to the deep-water Green Point section. A second problem was the assumption that the conodont succession at the Green Point section was dominated by reworked taxa (e.g., Miller and Flokstra, 1999; Miller et al., 2003). An additional problem arose when Terfelt et al. (2012) demonstrated that the selected biomarker *Iapetognathus fluctivagus* appeared higher in the Green Point section and above the appearance of planktic graptolites. Terfelt et al. (2012) also proposed additional horizons that could serve as boundary levels, but did point out that currently, the Cambrian–Ordovician boundary is fixed by the first appearance of *Iapetognathus preaengensis*. Miller et al. (2014) however rejected this interpretation and maintained that *Iapetognathus fluctivagus* is the correct marker species for the base of the Ordovician.

Zhou et al. (1984) were the first to propose the Xiaoyangqiao section, Dayangcha, as stratotype section for the Cambrian–Ordovician system boundary. It was recommended as a GSSP candidate for the base of the Ordovician System at the Calgary Plenary Session (Chen et al., 1985). At the Sixth International Symposium on the Ordovician System held in Sydney, Australia, in 1991, the Xiaoyangqiao section was accepted as the only candidate section for Global Cambrian–Ordovician Boundary Stratotype by the International Cambrian–Ordovician Working Group (ICOBWG I). However, the selection of *Iapetognathus fluctivagus* as marker for the base of Ordovician by the Working Group became crucial, because the taxon has not been recorded from the Xiaoyangqiao section and the ICOBWG II selected the Green Point section, Newfoundland, Canada, as the Global Stratotype Section and Point (GSSP) for the base of the Ordovician System in January 1999. The decision was approved by the International Subcommission on Ordovician Stratigraphy (ISOS) in September 1999 and the Commission on Stratigraphy (ICS) in November 1999, and finally ratified by the International Union of Geological Sciences (IUGS) in January 2000 (Cooper et al., 2001).

2. The Xiaoyangqiao section

The Xiaoyangqiao section (42°3′24″N, 126°42′21″E), Dayangcha, Hunjiang, Jilin Province, NE China is situated along the NW side of a small rivulet — a tributary of the Hunjiang River — 2.5 km NNE of the town of Dayangcha (Fig. 1). Access by car is

approximately 40 minutes from Baishan, and ca. 10 minutes from Jiangyuan, and 5 minutes drive from the town of Dayangcha; alternatively, the train from Baishan takes about 30 minutes.

The lithology, fossil record and stratigraphy of the upper Cambrian (Stage 10, Furongian Series) and Lower Ordovician (Tremadocian) succession of the Xiaoyangqiao section were studied by Kuo et al. (1982), Zhou et al. (1984), Chen et al. (1983, 1985, 1988, 1995), Chen (1986), and Zhang et al. (1996). The fauna comprises acritarchs, conodonts, graptolites and trilobites in high variety and abundance. Erdtmann (1986), Lin (1986), Wang and Erdtmann (1987), and Zhang and Erdtmann (2004) studied the graptolites from the section. The conodonts have been documented by Chen et al. (1985) followed by Chen and Gong (1986) with additional information by Nowlan and Nicoll (1995) and Nicoll et al. (1999). Yin (1985, 1986, 1995) described the acritarch assemblages, and Qian (1986) described the trilobite fauna. Chen and Zhang (1986), Zhang (1986), and Zhang and Chen (1986) provided details on the succession and the depositional environment and Wang and Yang (1986) investigated the clay composition of the sediments. Chen et al. (1986) described the distribution of rare earth elements in the succession. Yang et al. (1986) estimated an uppermost Cambrian horizon (HBA 9B1) within the section to 500.7 ± 7.4 Ma based on Rb-Sr method. Ripperdan and Kirschvink (1992), Ripperdan et al. (1992), and Chen et al. (1995), independently, presented quite similar $\delta^{13}C$-isotope curves from the Xiaoyangqiao section. Ripperdan and Kirschvink (1992) and Ripperdan et al. (1992, 1993) introduced the magnetostratigraphy of the Cambrian–Ordovician beds and correlated the magnetostratigraphy to the biostratigraphy data.

2.1. Restudy of the Xiaoyangqiao section

In the past four years an international research group, consisting of seven geologists from China, Denmark and Germany re-sampled and re-studied the Xiaoyangqiao section and other relevant sections in the Dayangcha area. Three additional participants joined the project and expanded the international working group with one geologist from China and two geologists from Italy and Russia, respectively.

2.2. Material and methods

The Xiaoyangqiao section was measured between 2014 and 2016. Bed thicknesses (terminology after Tucker, 2003), colours, lithologies, textures, sedimentary structures, macrofossils and the stacking pattern of the strata were recorded in the field. Carbonates are

described according to the classification scheme of Dunham (1962), mixed siliciclastic-carbonate deposits are classified after Mount (1985) and siliciclastic sediments are classified after Wentworth (1922). The section was studied using an integrated litho-, bio-, sequence- and isotope stratigraphy approach.

The upper Cambrian–lowermost Ordovician succession (Fig. 2) was collected in detail or nearly bed-by-bed for conodont research. Two sample series (BH and DC) were collected, giving a total of 115 conodont-yielding samples. In addition, the original material described and published by Chen and Gong (1986) has been inspected and used for this investigation. The conodonts were studied under light stereomicroscope and some specimens are documented using the light microscope and Scanning Electron Microscope (SEM).

The new palynological data are obtained from 46 new samples (series DA) collected from either the same beds as for the conodonts, close to them, or just in-between the levels collected by Yin (1986). Some of the additional sampled levels yielded rich acritarch assemblages, allowing for the expansion of the previously known palynological characteristics of the studied strata.

Graptolite faunas are known from three levels/intervals in the Xiaoyangqiao section. In connection with the investigation of the faunas from the Xiaoyangqiao section, material from various localities (e.g., Quebec, Canada; western Newfoundland, Canada; Victoria, Australia) have been investigated and biostratigraphically compared with the Chinese faunas. This provided a better understanding of the preservation aspects and led to more precise biostratigraphical correlation of the earliest planktic graptolite faunas worldwide.

Carbon isotope analysis was carried out on the bulk carbonate fraction of 96 samples in the Cambrian–Ordovician interval from the Xiaoyangqiao section. The geochemical analysis was prepared and analyzed at the Isotopic Geochemistry Laboratory of the Wuhan Center of China Geological Survey, Wuhan, China. The carbon isotope ratios were measured using Gasbench II and ThermoFisher MAT253 mass spectrometer. The C-isotope values are reported in the standard δ notation in per mil (‰) relative to the PDB standard with a precision of 0.1‰.

The transgressive-regressive (T-R) sequence approach introduced by Embry and Johannessen (1992) is adopted here for the sequence stratigraphy approach. The transgressive-regressive approach uses the subaerial unconformity as the unconformable portion of the boundary, and the maximum regressive surface (MRS) as the correlative conformity. The T-R sequence approach is used due to the absence of subaerial unconformities in the section, which might otherwise be used as sequence boundaries. The

individual T-R sequences are bound by MRSs, not sequence boundaries of the traditional Exxon sequence stratigraphic model (cf. Catuneanu et al., 2009, 2011).

A single T-R sequence can be further divided into a fining-upward transgressive systems tract (TST) below, and a coarsening-upward regressive systems tract (RST) above, with the maximum flooding surface (MFS) being the mutual boundary. These are distinctive surfaces of non-deposition, sediment starvation and condensation that tend to cap the finest grained sediments of the TSTs and precede the onset of coarsening-upward cycles (RSTs).

All data provide the basis for the sequence stratigraphic arrangement introduced here and the T-R approach works well in more distal sections, which lack a subaerial erosional unconformity.

3. Geological context of the Xiaoyangqiao section of Dayangcha, Hunjiang, Jilin Province

3.1. Geological setting

The upper Cambrian–Lower Ordovician sedimentary successions accumulated on the stable North China Craton (NCC or Sino–Korean Craton, SKC; Fig. 1), which comprises most of North China and parts of the Korean Peninsula (Fig. 1; Zhu et al., 2012). The craton forms the core of the North China plate, which is one of the three Chinese peri-Gondwana terranes (i.e., North China, South China, and Tarim blocks; Meyerhoff et al., 1991; Torsvik and Cocks, 2016). Today, the North China Craton is bounded to the north by the Central Asian Orogenic belt (Altaids) (Meng et al., 1997; Zheng et al., 2013), to the west by the western Tethyan subdomain, and to the south by the Qinling–Tongbai–Hong'an–Dabie–Sulu Orogenic Belt (Li and Powell, 2001; Kusky et al., 2007; Xiao et al., 2009; Zhai and Santosh, 2013). The eastern margin is delineated by the Pacific subduction zone, which was formed by the collision with South China (Lee and Chough, 2011). Thus today, the North China block covers an area of about 1500 km from east to west and 1000 km from north to south (Meng et al., 1997).

The basement of the North China Craton is composed of Archean (Eastern block), with the oldest dated at 3800 Ma, and Palaeoproterozoic rocks (Western Block). A thick succession of Neoproterozoic to Palaeozoic sedimentary deposits unconformably overlies the basement (Zhao and Zhai, 2013; Zheng et al., 2013). The Cambrian–Ordovician platform succession, about 500 to 1000 m thick, is composed of carbonate shallow marine water deposits with intervals of extensive biostromal microbialites (Lee et al., 2012), some mixed

carbonate and siliciclastic and evaporites (gypsum), oolites and lime breccias that accumulated on the craton (Feng and Jin, 1994). A thicker package composed of mixed carbonates and siliciclastics was deposited in the median to outer shelf to slope setting of the southeastern margin of the North China (Fig. 1). The carbonate platform of eastern North China settled on a ramp-like margin during the late Cambrian–Early Ordovician. The median shelf siliciclastic-carbonate belt was in places rimmed seaward by a low stromatolite reef and the outer shelf carbonate platform was flanked seaward by a shale-rich outer detrital belt of the platform margin.

During the late Cambrian and Early Ordovician the North China plate occupied a tropical position and the sedimentary succession was deposited in an extensive epeiric sea (Meyerhoff et al., 1991; Fu, 1996, pp. 37–38; Fu and Lai, 1996, pp. 37–40; Meng et al., 1997). The North China Block drifted northward and was situated near the equator during the early Palaeozoic (Fu, 1996; Fu and Lai, 1996; Li and Powell, 2001; Burrett et al., 2014; Torsvik and Cocks, 2016). In the late Cambrian the palaeogeographical position of the North China block was within 10º of the equator, but in the latest Cambrian to earliest Ordovician it changed to the subaequatorial belt with hurricanes. This is seen in the increase of storm deposits, evaporites (gypsum), oolites and lime breccias in the uppermost Cambrian to lowermost Ordovician successions of the North China block (Liu and Zheng, 1998; Kwon et al., 2006). It was tectonically stable during most of the Cambrian, but a hiatus of variable magnitude across the Cambrian–Ordovician boundary is developed at many sites on the North China platform, which is interpreted as being caused by an uplift that occurred on the western margin of the North China plate. The Ordovician succession is interrupted due to the ‘Huaiyuan Movement’ forming a hiatus extending from the mid-late Floian (Early Ordovician) into the early Darriwilian (Liu et al., 1997; Wang et al., 2016; Zhen et al., 2016). Sedimentation on the North China plate returned in the Middle Ordovician and persisted into the early Late Ordovician. A second uplift caused the formation of a great hiatus and lower Upper Ordovician sedimentary rocks are disconformably overlain by an Upper Carboniferous to Lower Permian succession composed of marine and terrestrial deposits (Zheng et al., 2013).

3.2. Stratigraphy and succession

The Ordovician sedimentary rocks of the Dayangcha area form a succession characterized by marine mixed siliciclastic-carbonate, upward-deepening and upward shallowing cyclic sedimentation. These upper Cambrian to Lower Ordovician sedimentary rocks, very well exposed at the Xiaoyangqiao section, are here referred — informally — to

the Dayangcha beds (cf. Erdtmann, 1986; Fig. 1B). The underlying, mainly sedimentary carbonates and subordinate shales, exposed along the road in the Xiaoyangqiao lower section (XLS), immediately to the south of the Xiaoyangqiao composite section (XCS) (Fig. 1B), are referred to the Furongian Fengshan Formation (Zhang, 1962). The Lower Ordovician (Tremadocian) strata of the Yeli (or Yehli) Formation (Grabau, 1922) overlie the Dayangcha beds (Zhang, 1962; Wang et al., 1996). The Yeli strata are composed mainly of carbonate sedimentary rocks with only subordinate calcareous shale. The Yeli Formation is exposed in the other small rivulet immediately to the south of the Xiaoyangqiao section and along the new main road (Zhang and Erdtmann, 2004; Fig. 1B). The Xiaoyangqiao section and the westerly facing section with exposures of the Yeli Formation and situated just to the south of the Xiaoyangqiao section are together named the Xiaoyangqiao composite section (XCS) (Chen, 1986; Zhang, 1986; Fig. 1B).

3.2.1. Lithostratigraphy

The Dayangcha beds exposed at the Xiaoyangqiao section consist of mixed carbonate-siliciclastic sedimentary rocks, composed primarily of limestone, siltstone and shale, subordinate conglomerates and strata bound breccias that dip evenly from 21° to 48° to the northeast (Fig. 2).

The Dayangcha beds can be subdivided into four lithostratigraphic informal units (I–IV; Fig. 3).

3.2.1.1. Unit I

Unit I is composed of mixed shale, shale with thin limestone lenses and limestone beds. Unit I, ca. 11 m thick, comprises a series of upward deepening one metre-scale cycles but shows an increasing abundance of siltstone in the uppermost part of the unit and just below the capping limestone. In the unit the ratio carbonate: siliciclastic is about 1:1 with an increase up-section of the siliciclastic content. Unit I starts from middle of the Xiaoyangqiao low section (XLS), exposed along the road to Dayangcha (Fig. 1), and continues upwards from the base of the Xiaoyangqiao section; it terminates just below the reference level of the Xiaoyangqiao section (i.e., at 0 on Fig. 3). Trilobites, associated with some brachiopods, are present to common in the shale.

3.2.1.2. Unit II

This unit is dominated by carbonate deposition starting with shallow water carbonate into gradually increasing deeper water carbonates, commonly nodular, and minor interbedded shale (parted and ribbon limestone). This unit includes the prominent columnar stromatolite marker bed (1.4 to 1.6 m thick) slightly above the reference level. Unit II begins at –0.20 m and extends up to +7.10 m in the section (Figs. 2, 3). Trilobites are present in the unit.

Unit II represents a brief recovery of the carbonate factory on the platform with little input of siliciclastic material.

3.2.1.3. Unit III

Unit III is predominantly siliciclastic shale and siltstone interbedded with minor thin argillaceous, commonly nodular, limestone beds. Input of carbonate conglomerate and imbricated limebreccia horizons is recorded in the middle of the unit and a series of strata bound limebreccia beds characterizes the top of the unit. Glauconite becomes a characteristic component in the middle to upper part of unit III. Trilobites are frequent in unit III and the first planktic graptolite appears at the top of the unit (Figs. 2, 3). Unit III starts at +7.1 m and extends to +21.4 m and thus it is 14.3 m thick. Sponge spicules are common in the limestone.

The limebreccias are interpreted as storm generated deposits or tempestites produced by hurricanes (e.g., Kwon et al., 2006; Chen and Lee, 2013; Chen, 2014). The conglomerate bed probably was deposited by a debris flow. The presence of glauconite in the upper unit III signifies a depth of 150 to 200 m (e.g., Porrenga, 1967) and low deposition rate (Odin, 1988).

3.2.1.4. Unit IV

Unit IV comprises almost exclusively siliciclastic sedimentary rocks, composed of green, light grey shale to black shale, and grey to light grey siltstone and few fine-grained sandstone beds. Thin, flat lenticular carbonate beds may occur in the dark grey to black shale; a few beds of limestone are recorded at the top of the unit. Except for the black shale, glauconite is a common mineral in this member. The most significant macrofossils in unit IV are planktic graptolite assemblages. This unit extends from +21.4 m and up to the top of the exposed section (Fig. 3). Unit IV is at least 9.80 m thick: it is most likely thicker as the upper boundary of the unit has not been reached in the Xiaoyangqiao section.

3.2.2. Biostratigraphy

The biostratigraphy of conodonts and graptolites from the Xiaoyangqiao section is outlined below. The acritarchs are in an early stage of revision and biostratigraphic units are

presented informally. The trilobite succession, described by Chen et al. (1983, 1985, 1986, 1988), is presented here in abbreviated form.

3.2.3. Conodonts

The conodont fauna comprises eu- and paraconodonts, which are moderately to relatively abundant and the fauna is moderately diverse. In this investigation only the euconodonts are discussed. The specimens are only mildly altered showing a CAI of 1.5–2 suggesting that the host rocks were heated to a maximum of 140ºC (Epstein et al., 1977). The specimens are generally well preserved, but at times the specimens have broken cups and some are preserved with silt attached to the specimens.

3.2.3.1. Conodont evolutionary lineages

The investigated Cambrian–Ordovician interval in the Xiaoyangqiao section preserves the evolutionary succession of the conodont genus *Cordylodus* Pander, 1856 that derived from *Eoconodontus notchpeakensis* (Miller, 1969) (Figs. 4A, 5A). The *Cordylodus* lineage starts with *Cordylodus primitivus* Bagnoli, Barnes and Stevens, 1987 (Figs. 4B, 5B) succeeded by *C. proavus* Müller, 1959 (Figs. 4C, D, 5C, D), *C. caboti* Bagnoli, Barnes and Stevens, 1987 (Figs. 4E, F, 5E, F), *C. intermedius* Furnish, 1938 (Figs. 4I, J, 5I, J) and *C. lindstromi* Druce and Jones, 1971 (Figs. 4K–M, 5K–M). '*Cordylodus*' *andresi* Viira and Sergeeva in Kaljo et al., 1986 (see Viira et al., 1987) is recorded first at –2.4 m in the section and just below the appearance of *C. primitivus*. However, '*Cordylodus*' *andresi* is not phylogenetically connected with the genus *Cordylodus s.s.* (Bagnoli and Stouge, 2014).

In the Xiaoyangqiao section *Iapetognathus jilinensis* Nicoll, Miller, Nowlan, Repetski and Ethington, 1999 (Fig. 4O, P) represents a segment of the evolutionary lineage that yet has to be fully documented. It represents a derived taxon from its possible ancestor *Iapetognathus preaengensis* Landing in Fortey et al., 1982, which is the oldest known representative of the genus. Nowlan and Nicoll (1995) recorded 'an advanced species of *Iapetognathus*', from limestone beds in the upper Unit IV and exposed at top of the Xiaoyangqiao section, but these authors did not elaborate further on this occurrence. Here specimens of *Iapetognathus* have not been recorded from above the horizon with *Iapetognathus jilinensis*.

3.2.3.2. Conodont zonation

The complete evolutionary succession of *Eoconodontus–Cordylodus* allows for a precise biozonation in ascending order: the *Eoconodontus notchpeakensis*, *Cordylodus proavus*,

Cordylodus caboti, *Cordylodus intermedius*, and *Cordylodus lindstromi* bio (lineage) zones (Fig. 3). The overlying *Cordylodus angulatus* Zone has not been reached in the investigated section, but has been recorded from a closely located succession (Chen and Gong, 1986). The lineage zones used here are briefly outlined:

Eoconodontus notchpeakensis Zone is based on the FAD of the nominate species and ranges upward to the FAD of *Cordylodus proavus*. *Cambroistodus cambricus* Miller, 1980 and *C. minutus* (Miller, 1969) are characteristic and common associated species. The long-ranging *Teridontus nakamurai* (Nogami, 1967) is present throughout the zone. *Proconodontus muelleri* Miller, 1969 and *P. serratus* Miller, 1969 from below extend high into the zone. *Cordylodus primitivus* and '*Cordylodus*' *andresi* both appear in the upper to uppermost part of the zone; both range into the next zone.

The *Eoconodontus notchpeakensis* Zone is not completely developed in the Xiaoyangqiao section as the nominate taxon is already present in the basal beds of the section (Chen and Gong, 1986; this study). Chen and Gong (1986) defined the *Cambrooistodus* Zone for the same interval. *Cordylodus primitivus* is a potential taxon for the establishment of an additional zone or subzone (cf. Barnes, 1988) but is not introduced here.

The FAD of *Cordylodus proavus* defines the base of the *Cordylodus proavus* Zone in the Xiaoyanqguao section. *Cordylodus proavus* first appears in samples BD 8A/DC 32 at 0.6 m, i.e., a level, which is just below the prominent and characteristic stromatolite marker bed in the lower part of the Xiaoyangqiao section (Fig. 3). The upper boundary is at the FAD of *Cordylodus caboti*. Associated species include *Teridontus nakamurai* and *Fryxellodontus inornatus* Miller, 1969. The *C. proavus* Zone is 4.1 m thick in the Xiaoyangqiao section.

The *Cordylodus caboti* Zone is marked by the FAD of *Cordylodus caboti* and the top of the zone is at the FAD of *Cordylodus intermedius.* In the Xiaoyangqiao section *Cordylodus caboti* is first recorded in sample BD 11 at +4.6 m above the reference level. The associated fauna includes the species known from the *C. proavus* Zone and with the presence of *Cordylodus prion* Lindström, 1955 *sensu* Nicoll (1991) (Figs. 4Q, 5N). New taxa appearing in the very top of the zone include *Monocostodus sevierensis* Miller, 1980, *Semiacontiodus lavadamensis* Miller, 1969, *Hirsutodontus simplex* (Druce and Jones, 1971) and *Cordylodus drucei*, Miller, 1980 (Figs. 4G, H, 5G, H). The *C. caboti* Zone is 13.8 m thick in the Xiaoyangqiao section.

The *Cordylodus intermedius* Zone is defined by the FAD of the nominate species. The top is at the base of the overlying zone. The first record of *C. intermedius* in the Xiaoyangqiao section is in samples BH 23/DC 61; both samples were collected at +18.4 m. The top of the

zone is represented by sample, BD 28 at +21.4 m above the reference level and the zone is 3.0 m thick in the Xiaoyangqiao section. The zone includes several of the taxa from below, i.e., *Cordylodus drucei*, *Monocostodus sevierensis*, *Semiacontiodus* spp. and *Utahconus utahensis* (Miller, 1969). *Cordylodus prolindstromi* Nicoll, 1991 appears at +20.6 m (sample BD 26A) and is present with a short range within the uppermost part of the *C. intermedius* Zone (Fig. 3).

The *Cordylodus lindstromi* Zone is marked by the FAD of the eponymous species in sample BH 28 at +21.4 m above the reference level, which is ca. 50 cm above the FAD of *Rhabdinopora proparabola* (at +20.9 m). The upper boundary of the zone is not defined in the section as the marker species for the next zone, i.e., *Cordylodus angulatus*, has not been recorded in the section. *Cordylodus proavus*, *Cordylodus caboti*, and *Cordylodus intermedius* from below range into the zone.

In addition to the *Cordylodus* zonal species mentioned above the long-ranging *Teridontus nakamurai* is present; the characteristic *Iapetognathus jilinensis* Nicoll et al., 1999 appears in the lower part of the zone (in sample BD 29 at +21.7 m) and is present with a short range. *Utahconus beimodaoensis* Chui and Zhang in An et al., 1983 *sensu* Chen and Gong (1986) is a newcomer and appears in the uppermost part of the zone (i.e., at +30.2 m and within the *Anisograptus matanensis* graptolite Zone). This relatively unknown taxon may be useful for long distance correlation, as it has also been recorded from Laurentia (Landing et al., 1996; Landing and Westrop, 2006).

3.2.4. Graptolites

3.2.4.1. Graptolite evolutionary lineages

Rhabdinopora proparabola (Lin, 1986) (Fig. 6A–C) is the first planktic graptolite appearing in the succession of the Xiaoyangqiao section. It is recorded at +20.9 m above the base level (Fig. 3). This first planktic graptolite of the *Rhabdinopora* graptolite lineage appeared in the earliest Ordovician. Lin (1986) for the first time described the fauna of this level and differentiated nine species included in the three genera *Dictyonema*, *Heterograptus* and *Staurograptus*. All taxa are now interpreted to represent different growth stages and preservational aspects of a single species, *Rhabdinopora proparabola*. The species can be recognized by its three-vaned structure with an angle about 120° between them at the proximal end (Lin, 1986; Fig. 6A–C). None of the specimens can be shown to possess a nema and the three-vaned construction is directly attached to the tip of the sicula. The origin of this

feature is unclear, but *R. proparabola* might not be termed a nematophorous graptolite (cf. Kozłowski, 1971; Erdtmann, 1982), but it was likely a planktic taxon. There is no indication of an attachment disc and the peculiar three-vaned feature cannot have served as one, as it is too regularly developed. These vanes show a fusellar construction that starts at the tip of the sicula and later encroaches onto the sides of the sicula, covering it in part (Fig. 6A–C).

The next representative of the graptolite lineage is the revised *Rhabdinopora parabola* (Bulman, 1954) (Fig. 6D–G). *Rhabdinopora praeparabola* Erdtmann, 1982 is interpreted to represent juveniles of *R. parabola* and thus regarded as a junior synonym. *R. parabola* has a well-developed nema starting from the tip of the sicula. All more complete specimens from the Xiaoyangqiao section show that this nema shows multiple branching divisions (Fig. 6F, G) and is not comparable in construction to the vanes of *R. proparabola*. A number of taxa with branched nemata have been described from the Early Ordovician strata worldwide. As examples are here indicated *R. campanulatum* (Harris and Keble, 1928), *R. enigma* (Cooper and Stewart, 1979) and *R. scitulum* (Harris and Keble, 1928) from Australia and *R. flabelliformis belgica* (Bulman, 1970) from Belgium. It is currently unclear, whether these forms might be synonymous to *R. parabola* and a revision of these taxa is in progress. Previously, the density of stipes and dissepiments in the various species of the genus *Rhabdinopora* has been used to differentiate individual species statistically (Cooper et al., 1998), but this approach is problematic, because distortion and varying preservational aspects (Maletz et al., 2017). Thus, the identity of these, presumably earliest planktic graptoloids, has to be questioned in many cases.

3.2.4.2. Graptolite zonation

The *Rhabdinopora proparabola*, *R. parabola* and *Anisograptus matanensis* graptolite biozones are all well represented in the Xiaoyangqiao section.

The *R. proparabola* Zone is recorded at the appearance of *R. proparabola*, +20.9 m above the reference level. This is the only level at which the species has been recorded. All taxa described by Lin (1986) can be included in this single species as astogenetic variants or preservational aspects.

The *R. parabola* Zone is recorded 5.8 m above the appearance of *R. proparabola*. *R. parabola* is a common species in a short interval of about 10 cm in the Xiaoyangqiao section. All astogenetic stages from juveniles to mature and gerontic specimens have been described (Lin, 1986), but often specimens are fragmented. A number of specimens show enough relief

to investigate the thecal and proximal end construction of this taxon including the quadriradiate proximal development suggested by Cooper et al. (1998).

The *Anisograptus matanensis* Zone is marked by the appearance of the nominate species at +29.8 m (Figs. 3, 6H). A number of closely spaced horizons occur in which largely fragments of *Anisograptus matanensis* can be found. Specimens of *Rhabdinopora* have not been discovered in this interval. The top of the zone has not been recorded in the section.

3.2.5. Acritarchs

Early studies of acritarchs from the Xiaoyangqiao section demonstrated the occurrence of remarkably diverse and well-preserved palynomorphs of varying abundance throughout the sampled sedimentary succession (Yin, 1986). The palynological material was well described and illustrated and five acritarch assemblages were proposed from the latest Cambrian to earliest Ordovician (Yin, 1985, 1986, 1995). However, since 1995 significant taxonomical revisions and/or reconsiderations in acritarch taxonomy — especially of the Cambrian acritarch taxa — have been made. Therefore, comparison and correlation of the palynofloras described from the Xiaoyangqiao section with coeval assemblages from outside North China remained difficult.

This review revises some of taxonomical problems of the acritarch assemblages and also improves their distribution in the Cambrian–Ordovician interval recorded at the Xiaoyangqiao section (Fig. 7). The new study confirms that the distribution of acritarchs through the section is not homogeneous. Highly fossiliferous levels are followed by intervals with a gradual decrease in abundance and taxonomical diversity of the acritarchs. At some levels the acritarch assemblages are almost monospecific and represented predominantly by simple sphaeromorphs (*Leiosphaeridia*, *Granomarginata* (= *Annulum*), etc.). Probably the cyclic pattern, from favorable to poor, is one response to the repetitive changes of the depositional environment.

Three acritarch assemblages are distinguished in the upper Cambrian–Lower Ordovician succession of the Dayangcha beds (Fig. 7). Their correlation with the microflora described by Yin (1986) is shown in Fig. 9. Some of the suggested taxonomical changes concerning acanthomorph and diacrodian acritarchs (i.e., Dean and Martin, 1982; Moczydłowska, 1991; Raevskaya and Servais, 2009, with references) are adopted here.

3.2.5.1. Assemblage 1 (*Timofeevia phosphoritica–Polygonium–Solisphaeridium*)

Assemblage 1 is recorded in the lower part of the studied section, i.e., from –10.7 m to ca. –5.8 m (samples DA 1–DA 8) (Fig. 7). It is characterized by the association of simple acanthomorph acritarchs belonging to the *Polygonium–Solisphaeridium* (Fig. 8O) plexus together with *Timofeevia phosphoritica* Vanguestaine, 1978 (Fig. 8N) and less numerous representatives of the galeate taxa *Cymatiogalea* sp. and *Stelliferidium* sp. (Fig. 8). Some specimens of *Cristallinium*, *Multiplicisphaeridium* sp., ?*Comasphaeridium* sp., and *Granomarginata squamacea* Volkova, 1968 (= *Annulum squamaceum* (Volkova) Martin and Dean, 1983) are present in subordinate amount. Single fragments of ?*Retisphaeridium* sp., and possible *Eliasum* sp. are found in the sample DA 2, whereas representatives of ?*Tectitheca* are present in samples DA 3 and DA 4. The latter sample is characterized by a sharp increase in number of acritarchs, especially of the two genera *Timofeevia* and *Polygonium*. The occurrence here of some rare diacrodians, such as *Actinotodissus*, is considered to be stratigraphically important, confirming a late Furongian age (Volokova, 1990; Volkova and Kir'janov, 1995; Raevskaya and Servais, 2009). Similarly, the appearance of *Cymatiogalea* and *Stelliferidium* is confined to the Furongian Series (Volokova, 1990; Volkova and Kir'janov, 1995), whereas *Retisphaeridium*, *Eliasum*, *Comasphaeridium*, *Cristallinium*, *Timofeevia* and *Granomarginata* range from strata below. The gradual decrease in the acritarch abundance, in the samples DA 5–DA 8, is replaced by a new peak in sample DA 9 at –5.6 m, in which the next assemblages can be distinguished.

3.2.5.2. Assemblage 2 (*Vulcanisphaera africana–Ninadiacrodium*)

Assemblage 2 comprises almost all of the previous listed taxa but in varying quantities at different levels (i.e., samples DA 9–DA 24), however diacrodian acritarchs become remarkably more diverse and numerous. Apart from *Actinotodissus*, other genera occur, including *Acantodiacrodium*, *Dasydiacrodium*, *Ninadiacrodium*, and *Trunculumarium*. The most important late Furongian index species are *Ninadiacrodium caudatum* (Vanguestaine, 1973) Raevskaya and Servais, 2009 (Fig. 8I), *Dasydiacrodium obsonum* Martin in Martin and Dean, 1988 (in samples DA 11, DA 15, DA 15-1; Fig. 8L, M), *Ninadiacrodium dumontii* (Vanguestaine, 1973) Raevskaya and Servais, 2009 (samples DA 12 and DA 15), and *Trunculumarium* sp. (sample DA 14).

Acritarch diversity of the assemblage 2 is complemented by occurrence in the sample DA15 of some rare *Vulcanisphaera africana* (Deunff, 1961) Rasul, 1976 (Fig. 7H) and various galeates such as *Cymatiogalea* aff. *C. bouvardii* Martin, 1973 (Fig. 8E), *C. columellifera* (Deunff, 1961) Deunff et al., 1974, *C. cylindrata* Rasul, 1974, *Priscogalea* sp.,

Stelliferidium stelligerum (Gorka, 1967) Deunff et al., 1974, and *Stelliferidium* sp. In addition, *Globosphaeridium*, *Micrhystridium*, ?*Priscoteca* sp., and *Tasmanites* sp. are also present. The very rich interval, from –1.3 to –0.5 m (samples DA 15 and DA 16), is followed by almost barren strata. This change is associated with the transition from lithological unit I (mainly shale) to unit II (mainly carbonates) and evidently, environmental and/or preservational conditions favourable for acritarchs changed. Only rare small acanthomorphs and simple sphaeromorphs are still present. *Timofeevia* has its upper range within this assemblage.

3.2.5.3. Assemblage 3 (*Corollasphaeridium wilcoxianum*)

Assemblage 3 is recognized from the sample DA 25 by the appearance of the very distinctive palynomorph *Corollasphaeridium wilcoxianum* Martin in Dean and Martin, 1982 (Fig. 8A–C). This taxon is accompanied by *Acanthodiacrodium*, *Actinotodissus*, *Cymatiogalea*, *Globosphaeridium*, *Polygonium* and *Solisphaeridium*. The change in composition is clearly associated with the lithological change from unit II to unit III.

Several horizons within assemblage 3 are dominated by mainly one acritarch genus. *Granomarginata* is present in high numbers in samples DA 27, DA 30, DA 34, and DA 36; *Cymatiosphaera* in sample DA 28 and *Leiosphaeridia* is the predominant taxon in sample DA 39. The occurrence of *Cymatiogalea cuvillieri* (Deunff, 1961) Deunff, 1964 (Fig. 8F) in sample DA 37 confirms a proximity to the base of the Tremadocian (Raevskaya, 2000).

From sample DA 39 and to the top of the studied interval palynomorphs become very rare. Different morphotypes of *Corollasphaeridium* and related unidentified fragments occur together with few long-ranging taxa mentioned above (Section 3.2.5).

3.2.6. Trilobites

Trilobites in the Xiaoyangqiao section are present throughout the succession and found commonly in the shales (Fig. 7). Trilobites of the Dayangcha beds are of Asian-Australian affinity, but the fauna does share taxa with Laurentia. Among the taxa in the trilobite assemblage is the genus *Mictosaukia*, which is applied as zonal taxon in North, Northeast, and South China, and Western Australia for the uppermost Cambrian. *Leiostegium* is another widely distributed trilobite genus, which is known from Australia and North America and also useful for intercontinental correlation.

The biostratigraphic subdivision of the Dayangcha succession using trilobites is based on the zonation of Qian (1986) and summarized by Chen et al. (1988). Most of the zones were

termed assemblage zones, but they are based on the first appearance and co-occurrences of several taxa (Fig. 7). Qian (1986) introduced three zones and seven subzones. According to this, the association of trilobites is referred to the Furongian *Mictosaukia–Fatocephalus* and *Richardzonella–Platypeltoides* zones and the *Yosimuraspis* Zone spanning the uppermost Furongian and lowermost Tremadocian (Fig. 7).

4. Integration of biozones and acritarch assemblages

In the Xiaoyangqiao succession the *Cordylodus* lineage is recorded mostly from units I, II and III, and the graptolite fauna mostly from unit IV. However, representatives of the two fossil groups overlap in upper unit III and the zonal conodont index *Cordylodus lindstromi* almost coincides with *Rhabdinopora proparabola* in the top of unit III. The appearance of *Rhabdinopora proparabola* is recorded in a thin green shale horizon at +20.9 m and *Cordylodus lindstromi* first appears at +22.4 m, i.e., 0.5 m above the first graptolite horizon. The fact that the appearances of these two important species are very close provides a significant tie for zonal integration of these two important fossil groups and for intercontinental correlation. The *R. parabola* Zone is constrained to the *Cordylodus lindstromi* Zone, and the *Anisograptus matanensis* Zone begins within the *Cordylodus lindstromi* Zone.

Acritarch assemblage 1 is constrained to the *Eoconodontus notchpeakensis* Zone. Acritarch assemblage 2 initiates in the *E. notchpeakensis* Zone and extends upwards into the *Cordylodus caboti* Zone. Assemblage 3 from unit III coincides largely with the upper *Cordylodus caboti* Zone and all of the *C. intermedius* Zone.

The *Mictosaukia angustilimbata* and *Mictosaukia striata* trilobite subzones of the *Mictosaukia–Fatocephalus* Zone are recorded from the *Eoconodontus notchpeakensis* Zone. The *Alloleiostegium latilum–Pseudokoldiniodia perpetis* Subzone of the *Mictosaukia–Fatocephalus* Zone comprises all of the *Cordylodus proavus* Zone and extends into the lower *C. caboti* Zone. The *Richardsonella–Platypeltoides* Assemblage Zone is constrained to the upper *Cordylodus caboti* Zone. The following *Leiostegium* (*Manitouella*) Subzone of the *Yosimuraspis* Zone correlates clearly to the *Cordylodus intermedius* Zone and thus represents the top Cambrian. The *Yosimuraspis* (*Eoyosimuraspis*) and *Y.* (*Yosimuraspis*) subzones of the *Yosimuraspis* Zone are coeval to the *Cordylodus lindstromi* Zone, where the former is contained in the *R. proparabola* Zone and the latter is coeval to the *R. parabola* Zone. The base of the top *Yosimuraspis* (*Metayosimuraspis*) Subzone coincides closely with the

appearance of *Utahconus beimodaoensis* Churi and Zhang in An et al., 1983 *sensu* Chen and Gong (1986), which is from the basal part of the *A. matanensis* graptolite Zone.

The integration of the biozones and acritarch assemblages is summarized in Fig. 9.

5. Sequence stratigraphy

The succession exposed at the Xiaoyangqiao section was deposited on a calm terrigenous-dominated mid to outer shelf of the ramp. The shallow to deep water marine sediments accumulated on the mid shelf to the margin and edge of the shelf, which is indicated by the sedimentary rocks and the diverse macroinvertebrate and conodont faunas, and acritarch microfloras. The mid shelf facies association includes wackestone and locally authochthonous buildups. With increasing water depth the trilobite constituents gradually increase in abundance and siliceous sponge spicules become more numerous. The carbonate content decreases upward and fine-grained siliciclastic sedimentary rocks dominate the upper part of the succession, suggesting a progressive uplift of the source area and decrease of the carbonate factory activity.

Occasionally intercalated, thin- to medium-bedded limestones (wackestones to grainstones, limebreccias) marked by coarse-grained debris from the middle and inner shelf zones are interpreted as debris flows (tempestites), reflecting the storm-related export of shallow-marine material into the most distal and deepest shelf zones.

5.1. Sequence analysis

The succession exposed at the Xiaoyangqiao section is composed of meter-scale 'parasequences' deposited in marine subtidal to deeper water marine settings. The Xiaoyangqiao sequence is here arranged into five low frequency (3rd or higher order) cycles expressed by an alternation of (1) shale-limestone, (2) limestone, (3) shale, limestone and lime breccias and (4) siltstone-shale. Each of the four depositional sequences recognized in the whole exposed succession is bounded by the MRS that caps a succession of regressive sediments that coarsen upward as a result of decreasing accommodation space. The lower and upper sequences are not fully developed in the section whereas the middle sequences are fully preserved.

The biostratigraphic zonal boundaries usually are recorded within the lower transgressive parts of the sequences, close to but clearly above the MRS surfaces. Some biozones (i.e., graptolite biozones) are established immediately above the maximum flooding surface in the sequence.

5.1.1. Sequence A

Sequence A comprises lithological unit I. This lower depositional sequence is represented by the cyclically developed beds from the base of the section and up to the first limestone bed just above the siltstone bed at the top of unit I. Sequence A includes all the lower parasequences (Fig. 10). It consists of cyclic deposition composed of grey to dark grey shale and limestone. Basal portions of the parasequences are typically shale although some sequence bases are nodular to lenticular shale in outcrop. Middle portion of the parasequences is typically shale with nodular to lenticular limestone and shale grading upwards into fine-bedded shale. The upper portion of the parasequences is composed of wavy bedded argillaceous wackestone. The upper surface of the limestone is sometimes developed as a discontinuity surface with burrows.

Unit I represents a deepening-upward succession and is part of the transgressive system tract of sequence A. The MFS is displayed in the thickest shale layer with minor intervals of thin elongated limestone and shale (Fig. 10), which represents the regressive system tract of sequence A. The maximum regressive surface is just above the top siltstone bed (at –0.20 m).

Sequence A comprises the upper *Eoconodontus notchpeakensis* conodont Zone.

5.1.2. Sequence B

The second depositional sequence is represented by all the carbonate beds of unit II and includes the lower grey to dark grey shales of unit III. It is composed mainly of increasing deepening carbonate deposits in the lower half with an upward increase of the siliciclastic component. The prominent stromatolite marker horizon near the base is contained in the sequence. The transgressive system tract of sequence B is composed of carbonates with the maximum flooding surface within the upper shale unit (Fig. 10). The regressive system tract is composed of stacks of upwards coarsening shale to silt deposits. The maximum regressive surface is placed at the top of the cyclic siliciclastic facies and above the siltstone horizon at +15.10 m.

Sequence B comprises the *Cordylodus proavus* Zone and the lower to middle part of the *Cordylodus caboti* Zone.

5.1.3. Sequence C

Sequence C comprises the upper part of unit III. The basal part, composed of glauconite limemudstone and shale followed by increasing deepening deposits of shale-limestone,

represents the trangressive system tract. The position of the MFS is here placed within the shale (ca. at +19.3 m) (Fig. 10). The following series of limebreccias (tempestites) in the shale dominated facies (i.e., the background deposition) marks the RST. The MRS is placed at ca. +20.4 m, which is near the top of the brecciated beds. Internally, sequence C is composed of two parasequences: the lower parasequence comprises the strata from +15.1 m to +18.1 m and is capped by a debris flow, and the second parasequence comprises the strata from +18.1 m to +20.4 m.

Sequence C comprises the top of the *Cordylodus caboti* Zone and most of the *Cordylodus intermedius* Zone.

5.1.4. Sequence D

Sequence D consists of cycles composed of dark grey shale, black shale with thin flat lenses of limestone and dull grey, light grey to green siltstone.

The transgressive system tract is characterized by cycles of black shale and black shale with one cm or less thin lenses of limestone. The maximum flooding surface is recorded ca. at +23.0 m within an interval of black shale. The following regressive system tract is composed of cyclic wavy bedded siltstone to fine-grained sandstone interbedded with grey, green shale and minor black shale and shale with thin and flat limestone lenses.

In the Xiaoyangqiao section, the first planktic graptolite horizon and the appearance of *Cordylodus lindstromi* are recorded near the base of the transgressive system tract. Sequence D comprises the *Cordylodus lindstromi* conodont Zone (*pars*), *Rhabdinopora proparabola* and *R. parabola* graptolite zones.

5.1.5. Sequence E

This sequence is composed of limestone beds, some with ripple marks, interbedded with light grey shale/siltstone. Sequence E is not completely preserved in the Xiaoyangqiao section and only the TST is exposed in the top of the section. The base is placed on the top of the uppermost siltstone of sequence D, i.e., at +28.9 m.

Sequence E is contained within the uppermost part of the *Cordylodus lindstromi* conodont Zone and closely associated with the base of the *Anisograptus matanensis* Zone. *Utahconus beimodaoensis* Churi and Zhang in An et al., 1983 *sensu* Chen and Gong (1986) is also a good marker for the beginning of sequence E.

6. Sea-level changes

The deposits of the Xiaoyangqiao section display a series of sea-level changes, which are reflected in significant regressive events of global significance (cf. Haq and Schutter, 2008). Palaeoclimate played a significant role for the sea-level changes in the late Cambrian to Early Ordovician and a cooling stage interrupted the warm water carbonate deposition in the latest Cambrian (Stage 10, Furongian) (Frakes et al., 2005; Trotter et al., 2008; Runkel et al., 2010; Hearing et al., 2018). This caused a drop in the sea level, promoting a predominance of siliciclastic deposition in the latest Cambrian and earliest Ordovician.

The first significant sea-level lowstand or regressive event is recognized at the top of lithological unit I and just beneath the base of lithological unit II in the Xiaoyangqiao section. The top of unit I is upward coarsening from shale to siltstone and then changing into the overlying unit II composed of carbonate sedimentary rocks. Faunally, this regressive event corresponds to the end of the *Eoconodontus notchpeakensis* Zone and acritarch assemblage 3 followed by the *Cordylodus proavus* Zone.

The second regressive-transgressive transition is recognized within the lithological unit III. It is marked by the transition from the upward coarsening shale to siltstone regressive succession into the transgressive shale-limestone-conglomerate succession. This second regressive event occurs in the uppermost part of the *C. caboti* Zone preceeding the beginning of the *Cordylodus intermedius* conodont Zone.

The third regressive event in the section is seen in the upper unit III. It is marked by the upwards shallowing succession and characterized by condensed deposition. The regression event is displayed by a series of intraformational breccia beds, interpreted as tempestites, in the section. The regression event corresponds to the top of the *Cordylodus intermedius* (conodont) Zone.

The fourth regressive event is less prominent. It is seen in the higher part of unit IV. It is marked by the change from the upwards coarsening succession composed of the interbedded shale, shale with platey limestone and siltstone of the T-R sequence D and into the transgressive interbedded silt/shale and limestone beds of T-R sequence E. It is recorded within the upper *Cordylodus lindstromi* Zone, and contained within the lower *Anisograptus matanensis* Zone.

Internationally, the prominent regressive-transgressive sea-level change recorded at the top of unit I is coeval to the Lange Ranch lowstand or the global Lange Ranch Eustatic Event (LREE) of Miller (1992). The following regressive-transgressive event recognized in the section and found within unit III, correlates with the Basal House Lowstand of Miller (1984). The third regressive-transgressive event in the Xiaoyangqiao section corresponds to the

'Acerocare Regressive Event' of Erdtmann (1982, 1986) that is abbreviated ARE (cf. Cooper et al., 2001; Nicoll et al., 1992). The fourth regressive event recorded in the top of the Xiaoyangqiao section probably represents the Black Mountain Eustatic Event (BMEE) of Miller (1984) followed by the Stonehenge Transgression of Taylor et al. (1992; i.e., the T-R sequence E; but today most of these transgressive strata are covered at the Xiaoyangqiao section.

7. Chemostratigraphy

Three δ^{13}C-isotope curves have been prepared from the Xiaoyangqiao section (Ripperdan et al., 1993; Chen et al., 1995; this study, Fig. 11). Largely, the C-isotope curves resemble each other, although they diverge in detail (Fig. 11). Here the newly prepared C-isotope curve is used as reference.

7.1. $\delta^{13}C_{carb}$-isotope curves

The C-isotope curve shows three prominent and two smaller positive peaks. The most prominent negative-positive shift is recorded at the base of lithological unit II, i.e., from –1.40 m to +0.50 m in the section, where the values from +0.60 abruptly drop to +0.01, and then shifts to above +1.50 (Fig. 11). Chen et al. (1995) named this prominent negative-positive excursion 'Pre-*Cambroistodus* minimum' (TCM), but this name is abandoned because the genus *Cambroistodus* ranges across the excursion. The prominent excursion is characterized by the FAD of *Cordylodus proavus*, and is here assigned to the '*Cordylodus proavus* spike' (CPS) (Figs. 3, 11).

The following upward trend from +0.6 m and up to +14 m is generally negative; this trend was named the '*Cordylodus proavus* decline' (CPD) by Chen et al. (1995). A negative-positive excursion from +4.9 m to +7.1 m coincides with the gradual facies change from limestone to shale within unit II.

The following long negative trend from above the '*Cordylodus proavus* spike' (CPS) positive spike extends up to ca. 14 m where a shift towards the positive at ca. +14.0 m coincides with the MRS surface of sequence B. The prominent positive rise from ca. +16.3 m to ca. +17.3 m is very characteristic as also observed by Ripperdan et al. (1993) and Chen et al. (1995); the latter authors named this positive peak 'the *Hirsutodontus simplex* spike' (HSS). This name is maintained and applied here, because the positive excursion is clearly associated with the presence of *Hirsutodontus simplex* in the section (Figs. 3, 11).

The $\delta^{13}C_{carb}$-isotope curve changes sharply towards the negative, forming a negative peak at ca. +18.4 m (= no. 1, Fig. 11) above which a series of closely spaced negative-positive C-isotope excursions is recorded (Fig. 11). Chen et al. (1995) named the short interval from +19.0 m to +19.7 m the 'Basal *Cordylodus lindstromi* fluctuations' (BCLF), a term that is abandoned here because the FAD of *C. lindstromi* is recorded above this excursion in the section (Figs. 3, 11). The negative termination of the 'zig-zag' pattern (no. 2, Fig. 11) is characteristic; it is followed by a positive trend culminating in the large positive spike above the first planktic graptolite at +21.30 m (no. 3, Fig. 11) and within the TST of sequence C. This positive spike represents the first large, positive C-isotope excursion in the Early Ordovician that corresponds to the 'Rise of Planktic Graptolites' (see Section 8.1.2). In the Xiaoyangqiao section, *Rhabdinopora proparabola* occurs at the positive rise towards the first large, positive C-isotope excursion (no. 3, Fig. 11) and the peak nearly coincides with the FAD of *Cordylodus lindstromi.* Upsection, the C-isotope curve displays a second but slightly smaller positive peak at +22.9 m (no. 4, Fig. 11), coinciding with the MFS of sequence D. A gentle positive trend is noted upwards with a culmination peak at ca. +27.8 m (no. 5, Fig. 11). This broad positive culmination is followed by the appearance of *Anisograptus matanensis* in the Xiaoyangqiao section.

7.2. REE geochemical anomaly

The analysis for REE and other trace elements using brachiopod apatite in the section recorded a prominent REE anomaly or positive spike peaking at +19.5 m (Chen et al., 1986). This peak is recorded in the upper part of lithological unit III slightly above the MFS of sequence C in the section. It also coincides with the characteristic 'zig-zag' pattern of the C-isotope curve recorded within the *Cordylodus intermedius* Zone (Chen et al., 1995; this study; Fig. 11).

7.3. Magnetostratigraphy

The magnetic polarity pattern for the Cambrian–Ordovician transition has been documented for the entire Xiaoyangqiao section (Fig. 11; Ripperdan and Kirschvink, 1992; Ripperdan et al., 1992, 1993; Chen et al., 1995). Two normal-polarity zones and one reversed-polarity zone are identified in the section. The lower period of normal polarity is represented by the strata referred to lithologic unit I, with one single short reversal-polarity at –6.1 m (Fig. 11). This period of normal polarity is assigned to the *Eoconodontus notchpeakensis* Zone although the interval from the base of the section to –6.2 m is mainly

without data (cf. Ripperdan et al., 1993; Chen et al., 1995, table 2). A shift from the normal- to reversed-polarity zone is recorded at –5.9 m and the period with the reverse-polarity is represented by the strata of the lithologic units II and III. This reverse period corresponds to the *Cordylodus caboti* and *Cordylodus intermedius* zones. The return to a period with normal polarity at ca. +20.6 m in the Xiaoyangqiao section is abrupt and the shift to the normal polarity zone coincides closely with the sequence D boundary followed by the appearance of *Rhabdinopora proparabola* (i.e., at +20.9 m). The normal-polarity zone comprises the strata of lithologic unit IV and up to the top of the exposed strata in the Xiaoyangqiao section. This period comprises the *Cordylodus lindstromi* conodont Zone and the *Rhabdinopora proparabola*, *R. parabola* and *Anisograptus matanensis* graptolite zones (Figs. 3, 11; Chen et al., 1995, table 2).

8. Correlation with the Green Point GSSP section

One purpose here is to demonstrate that the detailed data obtained from the Xiaoyangqiao section allow for precise correlation, using multidisciplinary approach, with the Green Point GSSP section, Newfoundland, Canada.

8.1. The Green Point GSSP section

The information from Green Point GSSP section for the global Cambrian–Ordovician boundary includes biostratigraphy and geochemical data. The Green Point GSSP section was logged in detail by James and Stevens (1986), who referred the succession to the Green Point Formation (with two members) of the Cow Head Group (Figs. 12, 13). Smaller lithological units were referred to units 19 to 28 (also labelled ‘beds’ by some authors) in the section (Figs. 12, 13). Tripathy et al. (2014) provided a radiometric age at 484 ± 16 Ma, based on Re-Os isotopes, for the Green Point GSSP horizon, which is within unit 23.

The conodonts have been studied in great detail and fully described by Bagnoli et al. (1987) and Barnes (1988); additional information is provided by Terfelt et al. (2012) and Stouge et al. (2017). The graptolites in the Green Point section were described by Erdtman (1988) and Cooper et al. (1998) and summarized by Cooper et al. (2001).

8.1.1. Biostratigraphy and correlation

Here, the conodonts and graptolites are used for the biostratigraphical correlation of the Xiaoyangqiao section with the Green Point GSSP section. The *Cordylodus caboti*, *Cordylodus intermedius* and *Cordylodus angulatus* conodont zones are well constrained in the

Cambrian–Ordovician transitional beds, exposed at the Green Point GSSP section (Bagnoli et al., 1987; Barnes, 1988; Cooper et al., 2001; Terfelt et al., 2012; Fig. 12). The base of the upper Cambrian *C. caboti* Zone at Green Point has not yet been defined in the section, whereas *Cordylodus intermedius*, i.e., the nominate species for the uppermost Cambrian conodont zone, is first recorded from unit 22. The *C. intermedius* Zone extends to the FAD of *Iapetognathus preaengensis* in unit 23. *Iapetognathus preaengensis* (previously *I. fluctivagus* in Cooper et al., 2001; cf. Terfelt et al., 2012) is the biomarker for the GSSP and its FAD defines the base of the Ordovician System (Terfelt et al., 2012). The *Cordylodus angulatus* conodont Zone is recorded from unit 27, ca. 11 m above the GSSP. *Cordylodus lindstromi* has not been positively identified from the Green Point GSSP section.

In the Green Point section the first record of planktic graptolites is from unit 25, where *Rhabdinopora parabola* is recorded, associated with *Staurograptus dichotomus* Emmons, 1855. Previously, the beds of unit 25 were subdivided into the *R. praeparabola* and *R. parabola* zones (Erdtmann, 1986; Cooper et al., 1998, 2001), but the two biozones are here reduced to one zone. The *Anisograptus matanensis* Zone is present in the upper part of unit 26 and the base of this zone is below the base of the *Cordylodus angulatus* conodont Zone (Bagnoli et al., 1987; Barnes, 1988; Cooper et al., 2001).

New biostratigraphical information from the Green Point GSSP section includes three radiolarian assemblages, which are recorded from the units 18, 23, 25 and 26 (Won et al., 2005; Maletz, 2011; Pouille et al., 2014) (Figs. 13, 14). The late Cambrian radiolarian assemblage recorded from unit 18 is referred to the *Ramuspiculum*? assemblage. The next *Protoentactinia kozuriana* assemblage appears high in unit 23 and extends into unit 25, thus marking the base of the Ordovician System (Pouille et al., 2014). New taxa appear in unit 26 and this fauna is referred to the *Paraechidnina nevadensis* assemblage, which extends into the *C. angulatus* Zone according to Kozur et al. (1996). The radiolarian assemblages can be tied to the conodont and graptolite zonation (Fig. 13). The characteristic distribution of the radiolarian assemblages in the Cambrian–Ordovician boundary interval shows that this microfossil group has a great potential for identification of the Cambrian–Ordovician boundary and for international correlation.

Trilobites and brachiopods are rare but occur in the conglomerate layers (i.e., *Symphysurina cleora* and *Nanorhis hamburgensis* in unit 19 and *Symphysurina* cf. *brevis* in unit 25; James and Stevens, 1986).

The interval from unit 18 and up to the upper unit 22 correlates with the *C. caboti* Zone of the Xiaoyangqiao section. The upper unit 22 to the lower part of unit 23 correlates with the

Cordylodus intermedius Zone in the Xiaoyangqiao section. The graptolite zones including the revised *Rhabdinopora parabola* Zone in unit 25 and *Anisograptus matanensis* Zone in the uppermost part of unit 26 correlates with the two graptolite zones of the same names in the Xiaoyangqiao section.

The GSSP and the FAD of *Iapetognatus preaengensis* cannot be correlated biostratigraphically to the Xiaoyangqiao section due to the absence of the marker species in the Xiaoyangqiao section. The characteristic species *Iapetognathus jilinensis* from the Xiaoyangqiao section, occurring above the appearance of *Rhabdinopora proparabola* and in the *Cordylodus lindstromi* Zone, has not been recorded from Green Point section. Barnes (1988) and Cooper et al. (2001) noted that the GSSP level should be marked by the appearance of *Cordylodus lindstromi s.l.*, but this taxon has not been well documented and the presence of *C. lindstromi* (or *C. lindstromi s.l.*) at this level still awaits to be confirmed.

8.1.2. Chemostratigraphy and matching of the isotope chemostratigraphy

Three C-isotope curves have been prepared from the Green Point section (Margaritz, 1991; Nowlan, 1995; Azmy et al., 2014; Stouge et al., 2017). The C-isotope curve shown by Cooper et al. (2001, fig. 4) is a general curve that is not derived from the Green Point section.

The precise and high-resolution $\delta^{13}C_{carb}$ profile of the Green Point Section (Azmy et al., 2014; Stouge et al., 2017) is in detail very similar to that recorded from the Xiaoyangqiao section (Chen et al., 1995; this study) and the succession of spikes can be identified (Fig. 15). Among the most prominent common features of the two $\delta^{13}C_{carb}$ profiles is the positive trend from unit 21 with a broad positive peak in unit 22 in the Green Point section. This same trend and positive peak matches precisely the positive excursion recorded in the Xiaoyangqiao section and annotated HSS (i.e., '*Hirsutodontus simplex* spike' of Chen et al., 1995). The succeeding strong negative shift in the lower part of the overlying unit 23 and ca. 1.8 m below the GSSP level (no. 1, Fig. 15) matches the similar negative shift recognized at +18.4 m in the Xiaoyangqiao section (no. 1, Fig. 11; see also Chen et al., 1995). The 'zig-zag' pattern that characterizes the overlying interval from the lower to middle part of unit 23 and immediately below the GSSP horizon (Azmy et al., 2014; Stouge et al., 2017) also provides a precise match to the similar 'zig-zag' development observed in the Xiaoyangqiao section. In both sections this 'zig-zag' pattern is recognized from within the *C. intermedius* Zone. The maximum negative peak (no. 2, Figs. 11, 15) is the same for the two sections and characterizes the top of the Cambrian System in the Green Point GSSP section (Cooper et al.,

2001; Azmy et al., 2014; Stouge et al., 2017) and accordingly also in the Xiaoyangqiao section.

In the Green Point section, the most prominent C-isotope positive peak, representing the largest positive isotope $\delta^{13}C_{carb}$ isotope excursion in the earliest Ordovician, is identified from the lower part of unit 25, ca. 4.5 m above the GSSP horizon (no. 3, Fig. 15). It coincides precisely with the base of the revised *Rbabdinopora parabola* Zone (i.e., *R. praeparabola* Zone of Cooper et al., 2001) in the Green Point section. In the Xiaoyangqiao section, and above the appearance of *R. proparabola*, the matching C-isotope maximum peak is barren of graptolites. The next higher C-isotope positive peak marks the *R. parabola* Zone in the Green Point section (no. 4, Figs. 12, 15). Upsection follows the positive peak that marks the base of the *Anisograptus matanensis* Zone (no. 5, Figs. 12, 15).

8.1.3. Geochemical anomalies

A geochemical REE anomaly has been detected in the Green Point GSSP section low within the 'zig-zag' excursions in unit 23 of the *Cordylodus intermedius* Zone (Azmy et al., 2014, fig. 6). This is identical and coeval to the Xiaoyangqiao section, where the REE geochemical anomaly is recorded from the *Cordylodus intermedius* Zone, as described above (section 7.2). This REE geochemical anomaly, first recognized in the Xiaoyangqiao section (Chen et al., 1986), is similar and coeval to the REE anomaly documented from the Green Point section (Azmy et al., 2014). The REE anomaly of Green Point section is recorded below the GSSP in the Green Point section.

8.1.4. Sea-level changes

The interval preserving the GSSP horizon is contained between the Basal House lowstand, the base of which is marked by the prominent conglomerate named unit 19 (Figs. 12, 15) and the 'Acerocare Regressive Event', which is expressed by the prominent brown-weathering dolomitic siltstone/limestone of unit 24. Like in the Xiaoyangqiao section, the shift is from a broad negative C-isotope excursion to the initiation of the largest C-isotope positive excursion.

The precise correlation and matching between the two sections is shown in Fig. 16.

8.1.5. The Cambrian–Ordovician boundary in the Xiaoyangqiao section

The similarity between the $\delta^{13}C_{carb}$ curves from the two sections, and constrained by the precise biozonal correlation, demonstrates — with confidence — that these curves provide

strong correlative potential. Based on the precise match of the pattern of the $\delta^{13}C_{carb}$ isotope curves between the Green Point GSSP section and the Xiaoyangqiao section it is possible to determine the precise level for the FAD of the planktic graptolite in the former and to identify the level equivalent to the Green point GSSP horizon in the latter.

In the Green Point section, the first planktic graptolite species *Rhabdinopora proparabola* has not been recorded or positively identified. However, the first planktic graptolite *R. proparabola* should be found from the top of unit 24 extending into the base of unit 25 in the Green Point section, i.e., from the transgressive part of the prominent brown weathering siltstone horizon (= unit 24) that represents the 'Acerocare Regressive Event' and at the initiation of the largest positive $\delta^{13}C_{carb}$ isotope excursion. A further implication of this match is that unit 25, i.e., a level ca. 5 m above the GSSP horizon, represents the *Cordylodus lindstromi* conodont Zone as it is identified in the Xiaoyangqiao section. *Cordylodus lindstromi*, as mentioned above (Section 8.1.2), has not been recorded from the Green Point section. The genus is represented mainly by *Cordylodus proavus*, *Cordylodus caboti* and *Cordylodus intermedius*, which all are long-ranging conodont species that have been recorded from unit 25 in the Green Point section (Fig. 12; Bagnoli et al., 1987; Barnes, 1988; Cooper et al., 2001; this study).

The position of the GSSP horizon in unit 23 is situated just above the prominent negative excursion (no. 2, Fig. 15) in the Green Point Section and above the REE geochemical anomaly in the *Cordylodus intermedius* Zone. In the Xiaoyangqiao section the Cambrian–Ordovician boundary horizon can be placed at ca. +19.8 m (± 0.2 m), which is approximately 1 m below the appearance of the first planktic graptolite at +20.9 m in Xiaoyangqiao section (Fig. 3).

9. Proposal of the Xiaoyangqiao section as an ASSP section for the base of the Ordovician System

The correlation and precise match of C-isotope curves between the Xiaoyangqiao section and the Green Point GSSP section presented here demonstrates — for the first time — that accurate correlation and match of the GSSP horizon for the global Cambrian–Ordovician boundary outside the Green Point section, western Newfoundland, Canada is indeed possible. This fact alone strongly justifies the recommendation of the Xiaoyangqiao section as AASP for the global Cambrian–Ordovician boundary.

The Xiaoyangqiao section fully satisfies the requirements for a GSSP/ASSP section set out in the revised Guidelines for the establishment of global chronostratigraphic standards (Salvador, 1994; Remane et al., 1996).

9.1. The following requirements are fulfilled:

1. The Xiaoyangqiao section is easily accessible.
2. The succession is well-exposed; it displays a continuous sedimentation, and the sedimentary rocks are nonmetamorphic and not affected by strong diagenesis.
3. The Xiaoyangqiao section lies within the Cambrian–Ordovician boundary protection zone, 2 km to NEE of the town of Dayangcha, 25 km northeast of Baishan City (Hunjiang), and 7–8 km east of Jiangyuan County.
4. The upper Cambrian to Lower Ordovician succession, 32 m of which are exposed at the Xiaoyangqiao section, preserves the complete Cambrian–Ordovician transition (e.g., Chen, 1986; this study).
5. The succession is richly fossiliferous including benthos, nekton, phyto- and zooplankton.
6. All conodont and graptolite species that are important and used for long-distance or intercontinental correlation across different facies, are well displayed in the section.
7. Numerous trilobites and prolific acritarch assemblages are recorded from the Xiaoyangqiao section (Yin, 1985, 1986, 1995; Qian, 1986; Chen et al., 1988; Zhang et al., 1996; Wang et al., 2016; this study).
8. The investigated Cambrian–Ordovician interval in the Xiaoyangqiao section preserves a complete evolutionary succession from *Eoconodontus notchpeakensis* to the conodont genus *Cordylodus* Pander, via *Cordylodus primitivus*. This evolutionary lineage allows for the establishment of a series of conodont lineage zones in ascending order: the *Eoconodontus notchpeakensis*, *Cordylodus proavus*, *Cordylodus caboti*, *C. intermedius* and *C. lindstromi* biozones. The overlying *Cordylodus angulatus* Zone is recorded from the closely located exposures just to the east of the Xiaoyangqiao section (Chen, 1986).
9. The planktic Ordovician graptolites preserved in the section are referred to the *Rhabdinopora proparapola*, *Rhabdinopora parabola* and *Anisograptus matanensis* biozones.

10. The species *Rhabdinopora proparabola* (Lin, 1986) in the Xiaoyangqiao section represents the first representative of the *Rhabdinopora* lineage and is not known with certainty from other regions, except from perhaps Argentina (Zeballo et al., 2005).
11. The data mentioned above are directly comparable with the faunal succession at Green Point GSSP section and solve the correlation problems of the Cambrian–Ordovician boundary as it is fixed in the Green Point GSSP section.
12. The Xiaoyangqiao section is suitable for chemostratigraphic and magnetostratigraphic dating and provides the precise match with the Green Point GSSP section.
13. The geochemical REE anomaly first recorded in the Xiaoyangqiao section (Chen et al., 1986) from the *Cordylodus intermedius* Zone has been identified also in the Green Point section (Azmy et al., 2014). Like in the Xiaoyangqiao section, the REE anomaly is recorded above the HSS and below the GSSP horizon within the *Cordylodus intermedius* Zone in the Green Point GSSP section.

10. Conclusions

This contribution presents and summarizes new data on the Cambrian–Ordovician boundary interval obtained from the important Xiaoyangqiao section in North China and combined with the information from the Green Point section, i.e., the global GSSP section for the Cambrian–Ordovician boundary. This interdisciplinary study clearly demonstrates the strengths of the Xiaoyangqiao section for intercontinental correlation. We therefore recommend the section as a global ASSP section for the Cambrian–Ordovician boundary in order to provide a robust basis for the identification of the global Cambrian–Ordovician boundary level (Fig. 17).

The new results from this study — using integrated bio-, sequence-, chemo- and magnetostratigraphy from the Xiaoyangqiao section, Dayangcha, China, allowing for detailed comparison with the Green Point GSSP section — demonstrate that (1) the first planktic graptolite, *Rhabdinopora proparabola*, is recorded from the Xiaoyangqiao section; (2) the FAD of *Cordylodus lindstromi* is just above the appearance of the earliest planktic graptolite *Rhabdinopora proparabola;* (3) the Cambrian–Ordovician boundary is situated between the eustatic global Basal House Lowstand and the eustatic global ‘Acerocare Regressive Event’; (4) the earliest Ordovician maximum positive $\delta^{12}C_{carb}$ isotope peak is recorded at the base of the *Rhabdinopora parabola* graptolite Zone; (5) the GSSP horizon representing the global Cambrian–Ordovician boundary lies immediately above a distinct negative excursion in the two investigated sections; (6) the prominent positive $d^{13}C_{carb}$ excursion named *Hirsutodontus*

simplex spike (= HSS; i.e., Chen et al., 1995) and the REE anomaly, within the *Cordylodus intermedius* Zone, lie immediately below the Cambrian–Ordovician boundary in both sections.

All the points mentioned above can be applied as proxies — globally — for the identification of the Cambrian–Ordovician boundary (Fig. 18).

Problems concerning the Cambrian–Ordovician boundary remain to be solved. The first problem is when Cooper et al. (2001) fixed the position and placed the 'Golden Spike' for the Cambrian–Ordovician boundary in unit 23 in the Green Point section, they also assigned *Iapetognathus fluctivagus* Nicoll et al., 1999 as the biomarker for the Cambrian–Ordovician boundary. However, this chosen biomarker for the GSSP horizon is not present at the GSSP horizon, but instead the horizon is represented by *Iapetognathus preaengensis* Landing in Fortey et al., 1982 as correctly identified by Barnes (1988) in the proposal for the GSSP of the Cambrian–Ordovician boundary. The genus as defined by Nicoll et al. (1999) is probably polyphyletic and the chosen biomarker is not as widely distributed as previously thought.

The second problem is that the first planktic graptolite, *Rhabdinopora proparabola*, is recorded only from the Xiaoyangqiao section, and not observed from the Green Point GSSP section. The equivalent position for this first graptolite horizon, using high-resolution carbon isotope stratigraphy, is here estimated to be represented by the top bed of unit 24 into lowermost beds of unit 25 (Figs. 12, 15) — a level that is below the first appearance of *R. parabola* and above the global 'Acerocare Regressive Event' (= unit 24 in the Green Point section). In the Green Point section this interval only yields graptolite fragments and long-ranging conodonts. The estimated *R. proparabola* level is ca. 4 m above the GSSP horizon in the Green Point section and ca. 1 m above the estimated level representing the Cambrian–Ordovician boundary in the Xiaoyangqiao section.

Acknowledgements

The authors are deeply indebted to China Ministry of Sciences and Technology and China Geological Survey for their financial support to the research project (No. 2015FY310100-7, No. DD20160120-04). We also gratefully appreciate the support to the research project by Chinese Commission of Stratigraphy and Wuhan Center of China Geological Survey (WCGS). The isotopic geochemistry Laboratory of WCGS analyzed rock collected samples and prepared the samples for microfossils. A grant from the Carlsberg Foundation, Copenhagen, Denmark covering the travel to China for Svend Stouge is

gratefully appreciated. Fieldwork by Jörg Maletz was supported by Grant MA 1269/7-1 of Deutsche Forschungsgemeinschaft (DFG).

Special thanks go the journal referees P. Ahlberg, C.R. Barnes, and an anonymous referee, who read the submitted manuscript and provided numerous suggestions and recommendations that all improved the final manuscript.

References

Albanesi, G.L.M., Giuliano, E., Pacheco, F.E., Ortega, G., Monaldi, R.,;1; 2015. Conodonts from the Cambrian Ordovician Boundary in the Cordillera Oriental, NW Argentina. Stratigraphy 12 (3–4), 237–256.

An, T.X., Zhang, F., Xiang, W.D., Zhang, Y.Q., Xu, W.H., Zhang, H.J., Jiang, D.B., Yang, C.S., Lin, L.D., Cui, Z.T., Yang, X.C.,;1; 1983. The Conodonts of North China and the Adjacent Regions. Science Press, Beijing, 223 pp. (in Chinese, with English abstract).

Azmy, K., Stouge, S., Brand, U., Bagnoli, G., Ripperdan, R.,;1; 2014. High-resolution chemostratigraphy of the Cambrian–Ordovician GSSP: Enchanced global correlation tool. Palaeogeography, Palaeoclimatology, Palaeoecology 409, 135–144.

Bagnoli, G., Stouge, S.,;1; 2014. Upper Furongian (Cambrian) conodonts from the Degerhamn quarry road section, southern Öland, Sweden. GFF 136 (3), 436–458.

Bagnoli, G., Barnes, C.R., Stevens, R.K.,;1; 1987. Lower Ordovician (Tremadocian) conodonts from Broom Point and Green Point, Western Newfoundland. Bollettino della Società Paleontologica Italiana 25 (2), 145–158.

Barnes, C.R.,;1; 1988. The proposed Cambrian–Ordovician Global Boundary Stratotype and Point (GSSP) in Western Newfoundland, Canada. Geological Magazine 125 (4), 381–414.

Barnes, C.R., Williams, S.H.;1; (Eds.), 1991. Advances in Ordovician Geology. Geological Survey of Canada, Paper 90-9, 336 pp.

Bassett, M.G., Dean, W.T.;1; (Eds.), 1982. The Cambrian–Ordovician Boundary: Sections, Fossil Distributions, and Correlations. National Museum of Wales, Geological Series 3, Cardiff, 227 pp.

Bulman, O.M.B.,;1; 1954. The graptolite fauna of the *Dictyonema* shales of the Oslo region. Norsk Geologisk Tidsskrift 33 (1–2), 1–40.

Bulman, O.M.B.,;1; 1970. A new *Dictyonema* fauna from the Salmien of the Stavelot Massif (with a preface by F. Geukens). Bulletin de la Societé belge Geologie, Paleontologie, Hydrologie 79, 213–224.

Burrett, C., Zaw, K., Meffre, S., Lai, C.K., Khositanount, S., Chaodumrong, P., Udchachon, M., Ekins, S., Halpin, J.,;1; 2014. The configuration of Greater Gondwana — evidence from LA ICPMS, U-PB geochronology of detrital zirkons from the Palaeozoic and Mesozoic of Southeast Asia and China. Gondwana Research 26, 31–51.

Catuneanu, O., Abreu, V., Bhattacharya, J.P., Blum, M.D., Dalrymple, R.W., Eriksson, P.G., Fielding, C.R., Fisher, W.L., Galloway, W.E., Gibling, M.R., Giles, K.A., Holbrook, J.M., Jordan, R., Kendall, C.G.St.C., Macurda, B., Martinsen, O.J., Miall, A.D., Neal, J.E., Nummedal, D., Pomar, L., Posamentier, H.W., Pratt, B.R., Sarg, J.F., Shanley, K.W., Steel, R.J., Strasser, A., Tucker, M.E., Winker, C.,;1; 2009. Towards the standardization of sequence stratigraphy. Earth-Science Reviews 92 (1–2), 1–33.

Catuneanu, O., Galloway, W.E., Kendall, C.G.C., Miall, A.D., Posamentier, W., Strasser, A., Tucker, M.E.,;1; 2011. Sequence stratigraphy: Methodology and nomenclature. Newsletters on Stratigraphy 44 (3), 173–245.

Chen, J.T.,;1; 2014. Surface and subsurface reworking by storms on a Cambrian carbonate platform: evidence from limestone breccias and conglomerates. Geologos 20 (1), 13–23.

Chen, J.T., Lee, L.S.,;1; 2013. Soft-sediment deformation structures in Cambrian siliciclastic and carbonate storm deposits (Shandong Province, China): Differential liquefaction and fluidization triggered by storm-wave loading. Sedimentary Geology 288, 81–94.

Chen, J.Y.,;1; (Ed.), 1986. Aspects of the Cambrian–Ordovician Boundary in Dayangcha, China. China Prospect Publishing House, Beijing, 410 pp.

Chen, J.Y., Gong, W.L.,;1; 1986. Conodonts. In: Chen, J.Y. (Ed.), Aspects of the Cambrian–Ordovician Boundary in Dayangcha, China. China Prospect Publishing House, Beijing, pp. 93–223.

Chen, J.Y., Zhang, J.,;1; 1986. Remark on sedimentary environment. In: Chen, J.Y. (Ed.), Aspects of the Cambrian–Ordovician Boundary in Dayangcha, China. China Prospect Publishing House, Beijing, pp. 35–49.

Chen, J.Y., Teichert, C., Zhou, Z., Lin, Y., Wang, Z., Xu, J.,;1; 1983. Faunal sequence across the Cambrian–Ordovician Boundary in northern China and its international correlation. Geological et Palaeontologica 17 (5), 1–15.

Chen, J.Y., Qian, Y.Y., Lin, Y.K., Zhang, J.M., Wang, Z.H., Yin, L.M., Erdtmann, B.-D.;1; (Eds.), 1985. Study on Cambrian–Ordovician Boundary Strata and Its Biota in Dayangcha, Hunjiang, Jilin, China. China Prospect Publishing House, Beijing, 139 pp.

Chen, J.Y., Wang, Y.X., Yang, J.D.,;1; 1986. Rare earth and other trace elements in biogenic apatite across the Cambrian–Ordovician boundary. In: Chen, J.Y. (Ed.), Aspects of the Cambrian–Ordovician Boundary in Dayangcha, China. China Prospect Publishing House, Beijing, pp. 61–71.

Chen, J.Y., Qian, Y.Y., Zhang, J.M., Lin, Y.K., Yin, L.M., Wang, Z.H., Wang, Z.Z., Yang, J.D., Wang, Y.X.,;1; 1988. The recommended Cambrian–Ordovician boundary stratotype of the Xiaoyangqiao section (Dayangcha, Jilin Province), China. Geological Magazine 125 (4), 415–444.

Chen, J.Y., Zhang, J.M., Nicoll, R.S., Nowlan, G.S.,;1; 1995. Carbon and oxygen isotopes in carbonate rocks within Cambrian–Ordovician boundary interval at Dayangcha, China. Acta Palaeontologica Sinica 34 (4), 393–409.

Cooper, R.A., Stewart, I.R.,;1; 1979. The Tremadoc graptolite sequence of Lancefield, Victoria. Palaeontology 22 (4), 767–797.

Cooper, R.A., Maletz, J., Wang, H., Erdtmann, B.-D.,;1; 1998. Taxonomy and evolution of earliest Ordovician graptoloids. Norsk Geologisk Tidsskrift 78 (1), 3–32.

Cooper, R.A., Nowlan, G.S., Williams, S.H.,;1; 2001. Global Stratotype Section and Point for base of the Ordovician System. Episodes 24 (1), 19–28.

Dean, W.T., Martin, F.,;1; 1982. The sequence of trilobite faunas and acritarch microfloras at the Cambrian–Ordovician boundary, Wilcox Pass, Alberta, Canada. In: Bassett, M.G., Dean,

W.T. (Eds.), The Cambrian–Ordovician Boundary: Sections, Fossil Distributions, and Correlations. National Museum of Wales, Geological Series 3, Cardiff, pp. 131–140.

Deunff, J.,;1; 1961. Un microplancton à Hystrichosphères dans le Tremadoc du Sahara. Revue de Micropaléontologie 4 (1), 37–52.

Deunff, J.,;1; 1964. Systématique de microplancton fossile à Acritarches; révision de deux genres de l'Ordovicien inférieur. Revue de Micropaléontologie 7 (2), 119–124.

Deunff, J., Gorka, H., Rauscher, R.,;1; 1974. Observations nouvelles et précisions sur les Acritarches a large ouverture polaire du Paleozoique inférieur. Geobios 7 (1), 5–18.

Druce, E.C., Jones, P.J.,;1; 1971. Cambro-Ordovician conodonts from the Burke River structural belt Queensland. Bureau of Mineral Resources, Geology and Geophysics, Bulletin 110, 1–159.

Dunham, R.,;1; 1962. Classification of carbonate rocks according to depositional textures. In: Ham, W.E. (Ed.), Classification of Carbonate Rocks — A Symposium. American Association of Petroleum Geologists, Memoir 1, 108–121.

Embry, A., Johannessen, E.,;1; 1992. T-R sequence stratigraphy, facies analysis and reservoir distribution in the uppermost Triassic and Lower Jurassic succession, western Sverdrup Basin, Arctic Canada. In: Vorren, T.O., Bergsager, E., Dahl-Stamnes, Ø.A., Holter, E., Johansen, B., Lie, E., Lund, T.B. (Eds.), Artic Geology and Petroleum Potential. Norvegian Petroleum Society, Special Publication 2, 121–146.

Emmons, E.,;1; 1855. American Geology, containing a statement of the principles of the science, with full illustrations of the characteristic American fossils also an atlas and a geological map of the United States. Part II. J. Munsell, Albany, 251 pp.

Epstein, A.G., Epstein, J.P., Harris, L.,;1; 1977. Conodont alteration — An index to organic metamorphism. United States Geological Survey Professional Paper 995, 1–27.

Erdtmann, B.-D.,;1; 1982. A reorganization and proposed phylogenetic classification of planktic Tremadoc (early Ordovician) dendroid graptolites. Norsk Geologisk Tidsskrift 62 (2), 121–145.

Erdtmann, B.-D.,;1; 1986. Review of lithofacies and graptolite-based biofacies of three critical Cambrian–Ordovician boundary stratotype sections. In: Chen, J.Y. (Ed.), Aspects of the Cambrian–Ordovician Boundary in Dayangcha, China. China Prospect Publishing House, Beijing, pp. 374–391.

Erdtmann, B.-D.,;1; 1988. The earliest Ordovician nematophorid graptolites: taxonomy and correlation. Geological Magazine 125, 327–348.

Feng, Z.Z., Jin, Z.K.,;1; 1994. Types and origin of dolostones in the Lower Palaeozoic of the North China Platform. Sedimentary Geology 93 (3–4), 279–290.

Fortey, R.A., Landing, E., Skevington, D.,;1; 1982. Cambrian–Ordovician boundary sections in the Cow Head Group, western Newfoundland. In: Bassett, M.G., Dean, W.T. (Eds.), The Cambrian–Ordovician Boundary: Sections, Fossil Distributions, and Correlations. National Museum of Wales, Geological Series 3, Cardiff, pp. 95–129.

Frakes, L.A., Francis, J.E., Syktus, J.I.,;1; 2005. Climate Modes of the Phanerozoic. Cambridge University Press, Cambridge, 274 pp.

Fu, K.,;1; 1996. Palaeogeography map of the Early Ordovician of China. In: Wang, H. (Ed.), Atlas of the Palaeogeography of China. Cartographic Publishing House, Beijing, pt. I, pp. 1–143 (in Chinese).

Fu, K., Lai, C.,;1; 1996. Explanation of the 'Palaeogeographic map of the Early Ordovician of China'. In: Wang, H. (Ed.), Atlas of the Palaeogeography of China. Cartographic Publishing House, Beijing, pt. II, pp. 1–85, and pt. III, 1–25 (in Chinese (pt. II), with English abstract (pt. III)).

Furnish, W.M.,;1; 1938. Conodonts from the Prairie du Chien (Lower Ordovician) of the upper Mississippi Valley. Journal of Paleontology 12 (4), 318–340.

Gorka, H.,;1; 1967. Quelque nouveaux acritarches des silexites du Trémadocien supérieur de la région de Kielce (Montagne de Ste. Croix, Pologne). Cahiers de Micropaléontologie 1 (6), 1–8.

Grabau, A.W.,;1; 1922. Ordovician fossils from North China. Palaeontology Sinica, Series B, No. 1, 1–127.

Haq, B.U., Schutter, S.R.,;1; 2008. A chronology of Paleozoic sea-level changes. Science 322 (5898), 64–68.

Harris, W.J., Keble, R.A.,;1; 1928. The *Staurograptus* bed of Victoria. Proceedings of the Royal Society of Victoria (New Series) 40 (2), 91–95.

Hearing, T.W., Harvey, T.H.P., Williams, M., Leng, M.J., Lamb, A.L., Wilby, P.R., Gabbott, S.E., Pohl, A., Donnadieu, Y.,;1; 2018. An early Cambrian greenhouse climate. Science Advances 4, 1–11.

James, N.P., Stevens, P.K.,;1; 1986. Stratigraphy and correlation of the Cambro-Ordovician Cow Head Group, western Newfoundland. Geological Survey of Canada, Bulletin 366, 1–143.

Kaljo, D., Borovko, N., Heinsalu, H., Hazanovits, K., Mens, K., Popov, L., Sergejeva, S., Sobolevskaja, R., Viira, V.,;1; 1986. The Cambro-Ordovician boundary in the Baltic Ladoga Clint Area (North Estonia and Leningrad Region, USSR). Proceedings of the Academy of Sciences of Estonian SSSR, Geology 35, 97–108 (in Russian, with English abstract).

Kozłowski, R.,;1; 1971. Early development stages and the mode of life of graptolites. Acta Palaeontologica Polonica 16 (4), 313–343.

Kozur, H.W., Mostler, H., Repetski, J.E.,;1; 1996. Well-preserved Tremadocian primitive Radiolaria from the Windfall Formation of the Antelope Range, Eureka County, Nevada, U.S.A. Geologisch-Paläontologische Mitteilungen Innsbruck 21, 245–271.

Kuo, H.C., Duan, J.E., An, S.L.,;1; 1982. Cambrian–Ordovician boundary in the North China Platform with description of trilobites. Journal of Jiling University, Earth Science Edition 3, 9–28 (in Chinese, with English abstract).

Kusky, T.M., Windley, B.F., Zhai, M.G.,;1; 2007. Tectonic evolution of the North China Block: from orogen to craton to orogen. Geological Society of London, Special Publication 280, 1–34.

Kwon, Y.K., Chough, S.K., Choi, D.K., Lee, D.J.,;1; 2006. Sequence stratigraphy of the Taeback Group (Cambrian–Ordovician), mideast Korea. Sedimentary Geology 192, 19–53.

Landing, E., Westrop, S.R.,;1; 2006. Lower Ordovician faunas, stratigraphy, and sea-level history of the middle Beekmantown Group, northeastern New York. Journal of Paleontology 80 (5), 958–980.

Landing, E., Westrop, S.R., Knox, L.,;1; 1996. Conodonts, stratigraphy, and relative sea-level changes of the Tribes Hill Formation (Lower Ordovician, East-central New York). Journal of Paleontology 70 (4), 656–680.

Lee, H.S., Chough, S.K.,;1; 2011. Depositional processes of the Zhushadong and Mantou formations (Early to Middle Cambrian), Shandong Province, China: roles of archipelago and mixed carbonate-siliciclastic sedimentation on cycle genesis during initial flooding of the North China Platform. Sedimentology 58, 1530−1572.

Lee, J.H., Chen, J.T., Chough, S.K.,;1; 2012. Demise of an extensive biostromal microbialite in the Furongian (late Cambrian) Chaomidian Formation, Shandong Province, China. Geosciences Journal 16 (3), 275–287.

Li, Z.X., Powell, C.M.,;1; 2001. An outline of the palaeo-geographic evolution of the Australasian region since the beginning of the Neoproterozoic. Earth-Science Reviews 53, 237–277.

Lin, Y.K.,;1; 1986. A new planktonic graptolite fauna. In: Chen, J.Y. (Ed.), Aspects of the Cambrian–Ordovician Boundary in Dayangcha, China. China Prospect Publishing House, Beijing, pp. 224–254.

Lindström, M.,;1; 1955. Conodonts from the lowermost Ordovician of south-central Sweden. Geologiska Föreningens i Stockholms Förhandlingar 76, 517–604.

Liu, J.B., Zheng, Z.C.,;1; 1998. Stacking patterns and correlation of meter-scale shallowing upward cycles in the Lower Ordovician carbonates in Pingquan and Qinglongshan, North China. Journal of the Geological Society of Japan 104 (5), 327–345.

Liu, J.B., Wang, Y., Qian, X.L.,;1; 1997. Two Ordovician unconformities in North China: Their origins and relationships to regional carbonate-reservoir characteristics. Carbonates Evaporites 12 (2), 177–184.

Magaritz, M.,;1; 1991. Carbon isotopes, time boundaries and evolution. Terra Nova 3, 251–256.

Maletz, J.,;1; 2011. Radiolarian skeletal structures and biostratigraphy in the Early Palaeozoic (Cambrian–Ordovician). Palaeoworld 20, 116–133.

Maletz, J.,;1; 2017. The identification of putative Lower Cambrian Radiolaria. Revue de Micropaléontologie 60, 233–240.

Maletz, J., Wang, X.F., Wang, C., Stouge, S., Yan, C.,;1; 2017. The earliest planktic graptolites: taxonony and correlation. In: Wang, X.F., Stouge, S., Maletz, J., Wang, C., Yan, C. (Eds.), Field Guide and Abstracts for the Dayangcah International Workshop on the Cambrian–Ordovician Boundary. Wuhan Center of China Geological Survey, Wuhan, pp. 64–65.

Martin, F.,;1; 1973. Les Acritarches de l'Ordovicien inférieur de la Montagne Noire (Hérault, Fance). Bulletin Institute Royal des Sciences Naturelles de Belgique 48 (10) (dated 1972), 61 pp.

Martin, F.,;1; 1983. Chitinozoires et Acritarches Ordoviciens de la plate-forme du Saint-Laurent (Québec et sud-est de l'Ontario). Geological Survey of Canada, Bulletin 310, 1–59.

Martin, F., Dean, W.T.,;1; 1982. The sequence of trilobite faunas and acritarch microfloras at the Cambrian–Ordovician boundary, Wilcox Pass, Alberta, Canada. In: Bassett, M.G., Dean, W.T. (Eds.), The Cambrian–Ordovician Boundary: Sections, Fossil Distributions, and Correlations. National Museum of Wales, Geological Series 3, Cardiff, pp. 131–140.

Martin, F., Dean, W.T.,;1; 1983. Late Early Cambrian and Early Middle Cambrian acritarchs from Manuels River, eastern Newfoundland. Geological Survey of Canada, Paper 83-1B, 353–363.

Martin, F., Dean, W.T.,;1; 1988. Middle and Upper Cambrian acritarchs and trilobite zonation at Manuels River and Random Island, Eastern Newfoundland. Geological Survey of Canada, Bulletin 381, 1–91.

Meng, X., Ge, M., Taylor, M.E.,;1; 1997. Sequence stratigraphy, sea-level changes and depositional systems in the Cambro-Ordovician of the North China carbonate platform. Sedimentary Geology 114, 189–222.

Meyerhoff, A.A., Kamen-Kaye, M., Chen, C., Taner, I.,;1; 1991. Stratigraphy, Palaeogeography and Tectonics. Kluwer Academic Publishers, Dordrecht, 188 pp.

Miller, J.F.,;1; 1969. Conodont fauna of the Notch Peak Limestone (Cambro-Ordovician), House Range, Utah. Journal of Paleontology 43, 413–439.

Miller, J.F.,;1; 1980. Taxonomic revisions of some Upper Cambrian and Lower Ordovician conodonts with comments on their evolution. University of Kansas, Paleontological Contributions 99, 1–39.

Miller, J.F.,;1; 1984. Cambrian and earliest Ordovician conodont evolution, biofacies, and provincialism. In: Clark, D.L. (Ed.), Conodont Biofacies and Provincialism. Geological Society of America, Special Paper 196, 34–68.

Miller, J.F.,;1; 1992. The Lange Ranch Eustatic Event: a regressive-transgressive couplet near the base of the Ordovician System. In: Webby, B.D., Laurie, J.R. (Eds.), Global Perspectives on Ordovician Geology. A.A. Balkema, Rotterdam, pp. 396–407.

Miller, J.F., Flokstra, B.R.,;1; 1999. Graphic correlation of important Cambrian–Ordovician boundary sections. Quo Vadis Ordovician — Short Papers of the Eigth International Symposium on the Ordovician System. Acta Universitatis Carolinae, Geologica 43 (12), 81–84.

Miller, J.F., Evans, K.R., Loch, J.D., Ethington, R.L., Stitt, J.H., Holmer, L., Popov, L.E.,;1; 2003. Stratigraphy of the Sauk III Interval (Cambrian–Ordovivian) in the Ibex area, Wesern Millard County, Utah and Central Texa. Brigham Young University Geology Studies 47, 21–118.

Miller, J.F., Repetski, J.E., Nicoll, R.S., Nowlan, G., Ethington, R.L.,;1; 2014. The conodont *Iapetognathus* and its value for defining the base of the Ordovician System. GFF 136 (1), 185–188.

Moczydłowska, M.,;1; 1991. Acritarch biostratigraphy of the Lower Cambrian and the Precambrian–Cambrian boundary in southeastern Poland. Fossils and Strata 29, 1–127.

Mount, J.,;1; 1985. Mixed siliciclastic and carbonate sediments: a proposed first-order textural and compositional classification. Sedimentology 32 (3), 435–442.

Müller, K.J.,;1; 1959. Kambrische Conodonten. Zeitschift der Deutschen Geologischen Gesellschaft 111, 434–485.

Nicoll, R.S.,;1; 1990. The genus *Cordylodus* and latest Cambrian–earliest Ordovician biostratigraphy. BMR Journal of Australian Geology and Geophysics 11, 529–558.

Nicoll, R.S.,;1; 1991. Differentiation of Late Cambrian–Early Ordovician species of *Cordylodus* (Conodonta) with biapical basal cavities. BMR Journal of Australian Geology and Geophysics 12 (3), 223–244.

Nicoll, R.S.,;1; 1992. Evolution of the conodont genus *Cordylodus* and the Cambrian–Ordovician boundary. In: Webby, B.D., Laurie, J.R. (Eds.), Global Perspectives on Ordovician Geology. A.A. Balkema, Rotterdam, pp. 105–113.

Nicoll, R.S., Nielsen, A.T., Laurie, J.R.,;1; 1992. Preliminary correlation of latest Cambrian to Early Ordovician sea level events in Australia. In: Webby, B.D., Laurie, J.R. (Eds.), Global Perspectives on Ordovician Geology. A.A. Balkema, Rotterdam, pp. 381–394.

Nicoll, R.S., Miller, J.F., Nowlan, G.S., Repetski, J.E., Ethington, R.L.,;1; 1999. *Iapetonudus* (n. gen.) and *Iapetognathus* Landing, unusual earliest Ordovician multielement conodont taxa and their utility for biostratigraphy. Brigham Young University Geology Studies 44, 27–101.

Nogami, Y.,;1; 1967. Kambrische Conodonten von China, Teil 2: Conodonten aus den hoch oberkambrischen Yencho-Schichten. Memoirs of the College of Science, University of Kyoto, Geology and Mineralogy, Series B 33 (4), 211–218.

Norford, B.S.,;1; 1991. The international working group on the Cambrian–Ordovician boundary: report of progress. In: Barnes, C.R., Williams, S.H. (Eds.), Advances in Ordovician Geology. Geological Survey of Canada, Paper 90-9, pp. 27–32.

Norford, B.S., Webby, B.D.;1; (Eds.), 1988. Cambrian–Ordovician boundary. Geological Magazine 125 (4), 323–463.

Nowlan, G.S.,;1; 1995. Variations in marine carbon isotope ratios ($\delta^{13}C$) through the Cambrian–Ordovician boundary interval. International Cambrian–Ordovician boundary working group. St. John's, Newfoundland (Canada), December, 1995 (unpublished).

Nowlan, G.S., Nicoll, R.S.,;1; 1995. Re-examination of the conodont biostratigraphy at the Cambrian–Ordovician Xiaoyangqiao section, Dayangcha, Jilin Province, China. In: Cooper, J.D. (Ed.), Ordovician Odyssey: Short Papers for the Seventh International Symposium on the Ordovician System. Pacific Section of Society for Sedimentary Geology (SEPM), Book 77, 113–116.

Odin, G.S.;1; (Ed.), 1988. Green Marine Clays. Development in Sedimentology, 45. Elsevier, Amsterdam, 444 pp.

Pander, C.H.,;1; 1856. Monographie der fossilen Fische des silurischen Systems der Russich-Baltischen Gouvernements. Akademie der Wissenschaften, St. Petersburg, 91 pp.

Porrenga, D.H.,;1; 1967. Glauconite and chamosite as depth indicators in the marine environment. Marine Geology 5 (5–6), 495–501.

Pouille, L., Danelian, T., Maletz, J.,;1; 2014. Radiolarian diversity changes during the Late Cambrian–Early Ordovician transition as recorded in the Cow Head Group of Newfoundland (Canada). Marine Micropaleontology 110, 25–41.

Qian, Y.Y.,;1; 1986. Trilobites. In: Chen, J.Y. (Ed.), Aspects of the Cambrian–Ordovician Boundary in Dayangcha, China. China Prospect Publishing House, Beijing, pp. 255–306.

Raevskaya, E.G.,;1; 2000. Akritarkhi i biostratigraphija verkhov kembrija-srednego ordovika severo-zapada Vostochno-Evropejskoj Platformy [Acritarchs and biostratigraphy of the uppermost Cambrian–Middle Ordovician of the northwestern part of the East-European Platform]. PhD Thesis, Saint Petersburg State University, 174 pp. (in Russian).

Raevskaya, E.G., Servais, T.,;1; 2009. *Ninadiacrodium*: a new late Cambrian acritarch genus and index fossil. Palynology 33 (1), 219–239.

Rasul, S.M.,;1; 1974. The lower Palaeozoic acritarchs *Priscogalea* and *Cymatiogalea*. Palaeontology 17 (1), 41–63.

Rasul, S.M.,;1; 1976. New species of the genus *Vulcanisphaera* (Acritarcha) from the Tremadocian of England. Micropaleontology 22 (4), 479–484.

Remane, J., Bassett, M.G., Cowie, J.W., Gohrbandt, K.H., Lane, H.R., Michelsen, O., Naiwen, W.,;1; 1996. Revised guidelines for the establishment of Global chronostratigraphic standards by the International Commission on Stratigraphy (ICS). Episodes 19 (3), 77–81.

Ripperdan, R.L., Kirschvink, J.L.,;1; 1992. Paleomagnetic results from the Cambrian–Ordovician boundary sections at Black Mountain, Georgina Basin, western Queensland, Australia. In: Webby, B.D., Laurie, J.R. (Eds.), Global Perspectives on Ordovician Geology. A.A. Balkema, Rotterdam, pp. 93–103.

Ripperdan, R.L., Magaritz, M., Nicoll, R.S., Shergold, J.H.,;1; 1992. Simultaneous changes in carbon isotopes, sea level, and conodont biozones within the Cambrian–Ordovician boundary interval at Black Mountain, Australia. Geology 20, 1039–1042.

Ripperdan, R.L., Magaritz, M., Kirschvink, J.L.,;1; 1993. Carbon isotope and magnetic polarity evidence for non-depositional events within the Cambrian–Ordovician boundary section near Dayangcha, Jilin Province, China. Geological Magazine 130 (4), 443–452.

Ruedemann, R.,;1; 1937. A new North American graptolite faunule. American Journal of Science 33 (193), 57–62.

Runkel, A.C., Mackey, T.J., Cowan, C.A., Fox, D.L.,;1; 2010. Tropical shoreline ice in the late Cambrian: Implications for Earth's climate between the Cambrian Explosion and the Great Ordovician Biodiversification Event. GSA Today 20 (11), 4–10.

Salvador, A.;1; (Ed.), 1994. International Stratigraphic Guide: A Guide to Stratigraphic Classification, Terminology, and Procedure. 2nd Edition. International Union of Geological Sciences and the Geological Society of America Boulder, Colorado, 214 pp.

Stouge, S., Bagnoli, G., McIlroy, D.,;1; 2017. Cambrian–Middle Ordovician Platform-slope Stratigraphy, Palaeontology and Geochemistry of Western Newfoundland. Geological Survey of Newfoundland and Labrador, Open File 012B/0692, 106 pp.

Taylor, J.F., Repetski, J.E., Orndorff, R.C.,;1; 1992. The Stonehenge Transgression: A rapid submergence of the central Appalachian platform in the Early Ordovician. In: Webby, B.D.,

Laurie, J.R. (Eds.), Global Perspectives on Ordovician Geology. A.A. Balkema, Rotterdam, pp. 409–418.

Terfelt, F., Bagnoli, G., Stouge, S.,;1; 2012. Re-evaluation of the conodont *Iapetognathus* and implications for the base of the Ordovician System GSSP. Lethaia 45, 227–237.

Torsvik, T.H., Cocks, L.R.,;1; 2016. Earth History and Palaeogeography. Cambridge University Press, Cambridge, 317 pp.

Tripathy, G.R., Hannah, J.L., Stein, H.S., Yang, G.,;1; 2014. Re-Os age and depositional environment for black shales from the Cambrian–Ordovician boundary, Green Point, western Newfoundland. Geochemistry, Geophysics, Geosystems 15, 1021–1037.

Trotter, J.A., Williams, I.S., Barnes, C.R., Lecuyer, C., Nicoll, R.S.,;1; 2008. Did cooling oceans trigger Ordovician biodiversification? Evidence from conodont thermometry. Science 321, 550–554.

Tucker, M.E.,;1; 2003. Sedimentary Rocks in the Field. Wiley and Sons, Chichester, 237 pp.

Vanguestaine, M.,;1; 1973. New acritarchs from the Upper Cambrian of Belgium. In: Vozzhennikova, T.F., Timofeev, B.V. (Eds.), Microfossils of the Oldest Deposits. Proceedings of the Third International Palynological Conference, Novosibirsk, 1971. Akademiya Nauk SSSR, Siberskoe Otdelenie, Institut Geoogii I Geofizikii, Izdatelstvo, Nauka, Moskva, pp. 28–31.

Vanguestaine, M.,;1; 1978. Critères palynostratigraphiques conduisant a la reconnaissance d'un pli couche revinien dans le sondage de Grand-Halleux. Annales de la Société Géologique de Belgique 100, 249–276.

Viira, V., Sergeeva, S., Popov, L.,;1; 1987. Samye rannie predstaviteili roda *Cordylodus* (Conodonta) iz severnoj Ehstonii i Leningradskoj Oblasti [Earliest representatives of the genus *Cordylodus* (Conodonta) from Cambro–Ordovician boundary beds of North Estonia and Leningrad Region]. Proceedings of the Academy of Sciences of the Estonian SSR, Geology 36, 145–153 (in Russian).

Volkova, N.A.,;1; 1968. Akritarkhi dokembrijskikh i kembrijskikh otlozhenij Estonii. Problematika pogranichnykh sloev rifeja i kembrija Russkoj platformy, Urala i Kazakhstana. [Acritarchs from Precambrian and Cambrian strata of Estonia. Problems on boundary beds of

the Riphean and Cambrian of the Russian Platform, Ural and Kazakhstan]. Trudy GIN AN SSSR 188, 34–37 (in Russian).

Volkova, N.A.,;1; 1990. Akritarkhi srednego i verkhnego Kembrija Vostochno-Evropeiskoj platformy [Middle and Upper Cambrian acritarchs of the East-European Platform]. Trudy 454, Nauka, Moscow, 115 pp. (in Russian).

Volkova, N.A., Kir'janov, V.V.,;1; 1995. Regional'naya stratigraphicheskaya skhema sredneverkhnekembrijskikh otlozhenij Vostochno Evropejskoj platformy [Regional stratigraphic scheme of the Middle–Upper Cambrian of the East European Platform]. Stratigraphy and Geological Correlation 3 (5), 66–74 (in Russian).

Wang, X.F., Erdtmann, B.-D.,;1; 1987. Zonation and correlation of the earliest Ordovician graptolites from Hunjiang, Jilin Province, China. Bulletin of the Geological Society of Denmark 35, 245–257.

Wang, X.F., Chen, X., Chen, X.H., Zhu, Z.Y.,;1; 1996. Stratigraphical Lexicon of China — The Ordovician System. Geological Publishing House, Beijing, 192 pp.

Wang, Z.C., Yang, J.D.,;1; 1986. Clay mineral composition aspects and relevant implication of diagenetic process. In: Chen, J.Y. (Ed.), Aspects of the Cambrian–Ordovician Boundary in Dayangcha, China. China Prospect Publishing House, Beijing, pp. 50–60.

Wang, Z.H., Zhen, Y.Y., Zhang, Y.D., Wu, R.C.,;1; 2016. Review of the Ordovician conodont biostratigraphy in the different facies of North China. Journal of Stratigraphy 46 (1), 1–16 (in Chinese, with English abstract).

Webby, B.D., Laurie, J.R.;1; (Eds.), 1992. Global Perspectives on Ordovician Geology. A.A. Balkema, Rotterdam, 513 pp.

Wentworth, C.K.,;1; 1922. A scale of grade and class terms for clastic sediments. The Journal of Geology 30 (5), 377–392.

Won, M.Z., Iams, W.J., Reed, K.,;1; 2005. Earliest Ordovician (early to Middle Tremadoc) radiolarian faunas of the Cow Head Group, western Newfoundland. Journal of Paleontology 79, 433–459.

Xiao, W.J., Windley, B.F., Yuan, C., Sun, M., Han, C.M., Lin, S.F., Chen, H.L., Yan, Q.R., Liu, D.Y., Qin, K.Z., Li, J.L., Sun, S.,;1; 2009. Paleozoic multiple subduction–accretion processes of the southern Altaids. American Journal of Science 309, 221–270.

Yang, Y.D., Wang, Y.X.., Tao, X.C.., Li, H.M.., Wang, Z.Z.,;1; 1986. Rb-Sr dating on the Cambrian–Ordovician boundary interval. In: Chen, J.Y. (Ed.), Aspects of the Cambrian–Ordovician Boundary in Dayangcha, China. China Prospect Publishing House, Beijing, pp. 72–82.

Yin, L.M.,;1; 1985. Acritarchs. In: Chen, J.Y., Qian, Y.Y., Lin, Y.K., Zhang, J.M., Wang, Z.H., Yin, L.M., Erdtmann, B.-D. (Eds.), Study on Cambrian–Ordovician Boundary Strata and Its Biota in Dayangcha, Hunjiang, Jilin, China. China Prospect Publishing House, Beijing, pp. 101–112.

Yin, L.M.,;1; 1986. Acritarchs. In: Chen, J.Y. (Ed.), Aspects of the Cambrian–Ordovician Boundary in Dayangcha, China. China Prospect Publishing House, Beijing, pp. 313–373.

Yin, L.M.,;1; 1995. Early Ordovician acritarchs from Hunjiang, Jilin and Yichang region, Hubei, China. Palaeontologica Sinica 185, New Series A, 12, 1–170 (in Chinese and English).

Zeballo, F.J., Albanesi, G.L., Ortega, G.,;1; 2005. Conodontes y graptolitos de las formaciones Alfarcito y Rupasca (Tremadociano) en el área de Alfarcito, Tilcara, Cordillera Oriental de Jujuy, Argentina Parte 2: Paleontología sistema. Ameghiniana 42 (1), 47–66.

Zhai, M.G., Santosh, M.,;1; 2013. Metallogeny of the North China Craton: link with secular changes in the evolving Earth. Gondwana Research 16 (2), 321–341.

Zhang, J.M.,;1; 1986. Description of sections. In: Chen, J.Y. (Ed.), Aspects of the Cambrian–Ordovician Boundary in Dayangcha, China. China Prospect Publishing House, Beijing, pp. 7–14.

Zhang, J.M., Chen, J.Y.,;1; 1986. Lithofacies sequence. In: Chen, J.Y. (Ed.), Aspects of the Cambrian–Ordovician Boundary in Dayangcha, China. China Prospect Publishing House, Beijing, pp. 15–34.

Zhang, J.M., Wang, H.F., Li, G.X., Chen, J.Y.,;1; 1996. Redescription of the Dayangcha section as a candidate for the Global Cambrian–Ordovician Boundary Stratotype, Jilin Province, China. Journal of Stratigraphy 20 (2), 81–103 (in Chinese, with English abstract).

Zhang, W.T.,;1; 1962. Ordovician of China. Symposium on Stratigraphy of China. Science Press, Beijing, 62 pp. (in Chinese).

Zhang, Y.D., Erdtmann, B.-D.,;1; 2004. Tremadocian (Ordovician) biostratigraphy and graptolites at Dayangcha (Baishan, Jilin, NE China). Paläontologische Zeitschrift 78 (2), 323–354.

Zhao, G.C., Zhai, M.G.,;1; 2013. Lithotectonic elements of Precambrian basement in the North China Craton: Review and tectonic implications. Gondwana Research 23, 1207–1240.

Zhen, Y.Y., Zhang, Y.D., Wang, Z.H., Percival, I.G.,;1; 2016. Huaiyuan Epeirogeny — Shaping Ordovician stratigraphy and sedimentation on the North China Platform. Palaeogeography, Palaeoclimatology, Palaeoecology 448, 363–370.

Zhen, Y.Y., Percival, I.G., Webby, B.D.,;1; 2017. Discovery of *Iapetognathus* fauna from far western New South Wales: towards a more precisely defined Cambrian–Ordovician boundary in Australia. Australia Journal of Earth Sciences 64 (4), 487–496.

Zheng, Y.F., Xiao, W.J., Zhao, G.C.,;1; 2013. Introduction to tectonics of China. Gondwana Research 23, 1189–1206.

Zhou, Z.Y., Wang, Z.H., Zhang, J.M.,;1; 1984. Cambrian–Ordovician boundary and the proposed candidates for stratotype in North and Northeastern China. In: Nanjing Institute of Geology and Palaeontology, Academia Sinica (Ed.), Cambrian–Ordovician Boundary (2). Anhui Science and Technology Publishing House, Hefei, pp. 1–62 (in Chinese).

Zhu, R.X., Yang, J.H., Wu, F.Y.,;1; 2012. Timing of destruction of the North China Craton. Lithos 149, 51–60.

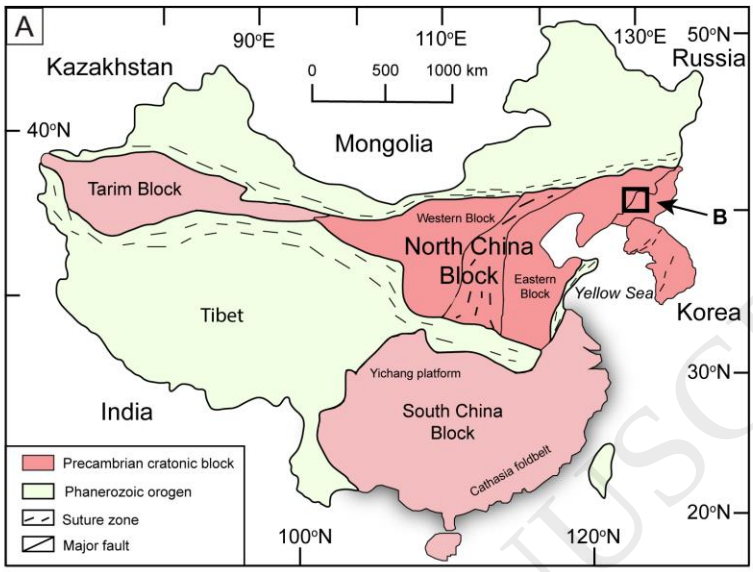

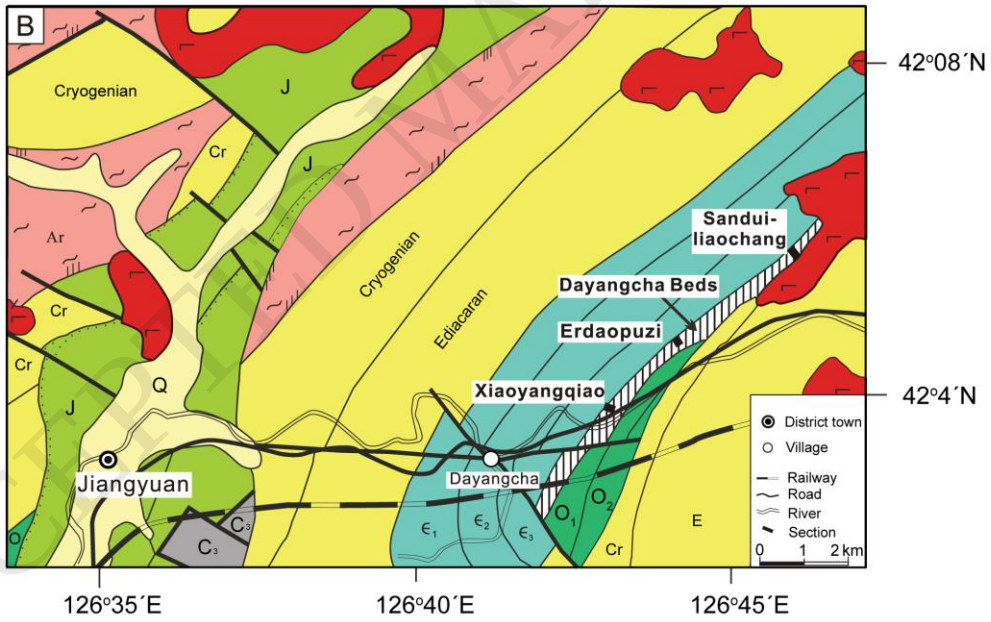

Legend

- Basement (Archean)
- Neoproterozoic: Cr = Cryogenian; E = Ediacaran
- Cambrian: ϵ_1 = lower; ϵ_2 = middle; ϵ_3 = upper
- Ordovician: O_1 = Lower; O_2 = Middle
- Carboniferous (C)
- Mesozoic: J = Jurassic
- Pleistocene (Q)
- Intrusive rocks
- Unconformity

Fig. 1. (A) Simplified tectonic map of the three main China plates (Tarim, North China and South China). (B) Geological and location map of the study area. The location of the significant Xiaoyangqiao, Erdaopuzi and Sanduiliaochang sections that are situated to the northeast of Dayangcha village is shown. The Baishan City, the main city of the Jiangyuan District, is located ca. 20 km southwest of Dayangcha (and outside (B)).

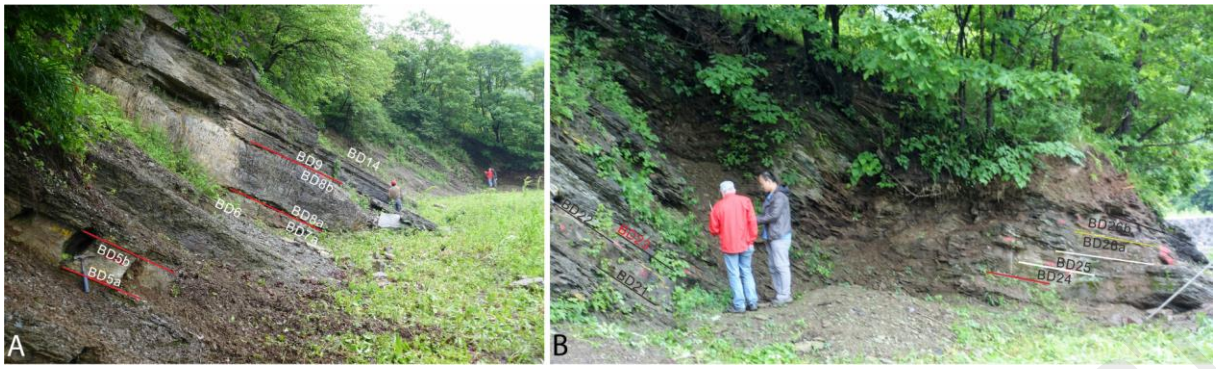

Fig. 2. Photos from the Xiaoyangqiao section (persons for scale). (A) Top of lithological units I and II. The base of lithological unit II is at BD 7a. Lithological unit II comprises BD 7a and extends to just above BD 14. The higher beds belong to lithological unit III. (B) Upper part of lithological unit III. The FAD of planktic graptolites is just above BD 26a at 20.9 m (to the right on the photo).

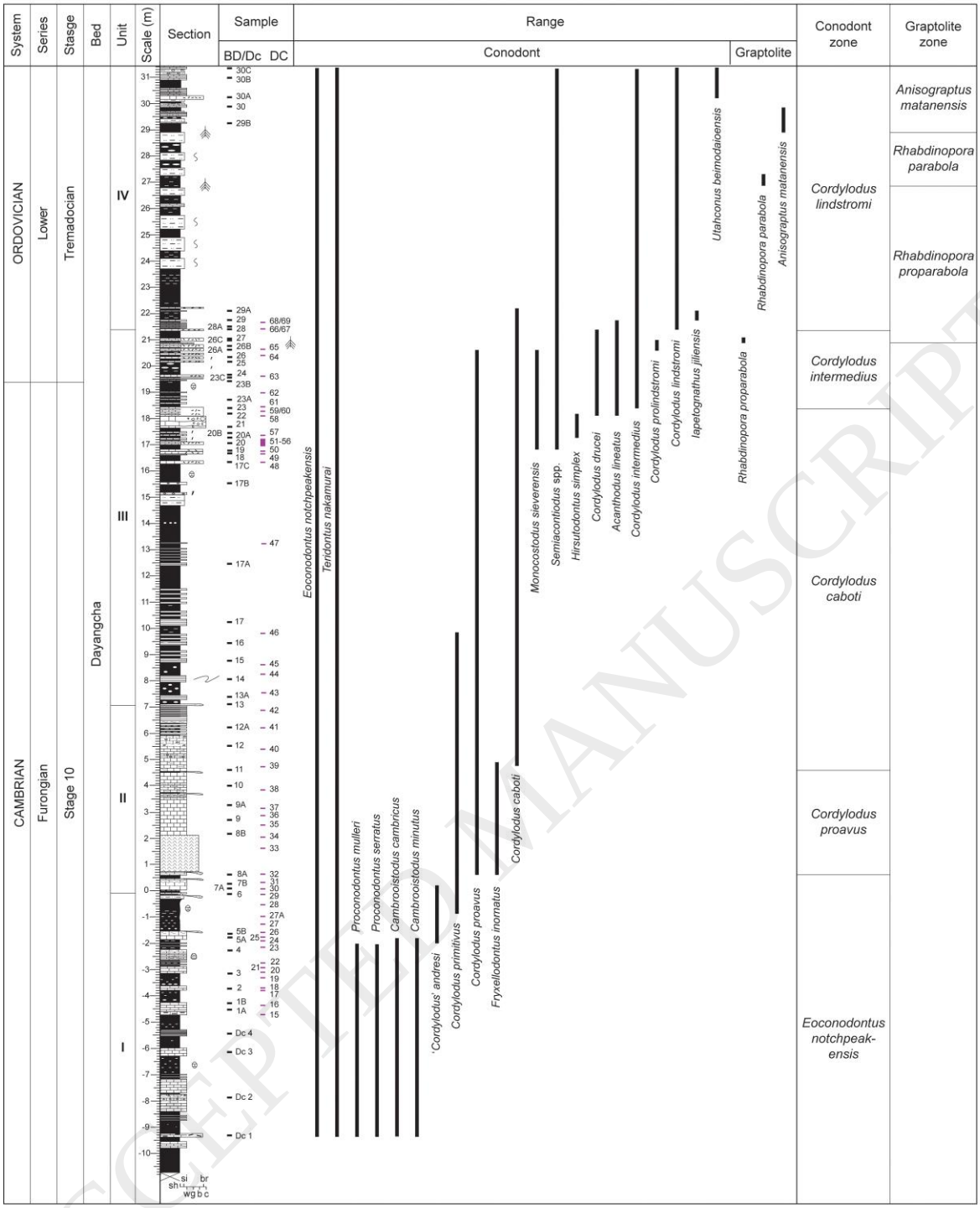

Fig. 3. Upper Cambrian to Lower Ordovician (Tremadocian) stratigraphy of the Xiaoyangqiao section and ranges of selected conodont and graptolite species. For legend, see Fig. 10. Abbreviations used for grainsize: sh = shale; si = siltstone; br = breccia; w = wackestone; g = grainstone; b = boundstone; c = conglomerate.

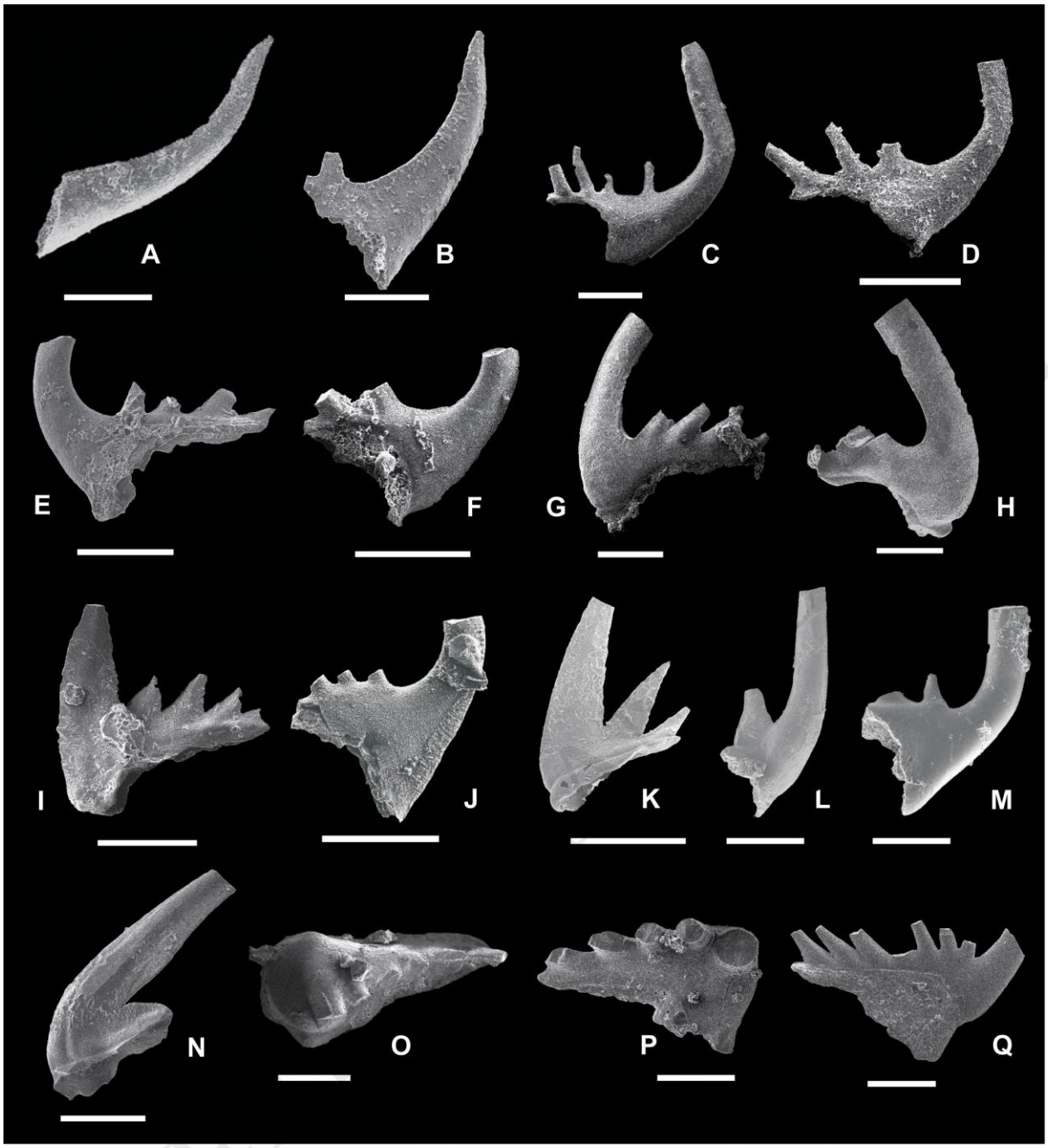

Fig. 4. Representative conodont species from the Xiaoyangqiao section. (A) *Eoconodontus notchpeakensis*, Miller, 1969, lateral view, BD 15, NIGP 174030. (B) *Cordylodus primitivus* Bagnoli, Barnes and Stevens, 1987, lateral view, BD 15, NIGP 174044. (C, D) *Cordylodus proavus* Müller, 1959, rounded elements, lateral view, BD 8B, NIGP 8B001 and NIGP 174034. (E, F) *Cordylodus caboti* Bagnoli, Barnes and Stevens, 1987, rounded elements, lateral view; (E) BD 23A, NIGP 23A001; (F) BD 22, NIGP 174017. (G, H) *Cordylodus drucei* Miller, 1980, outer lateral view, BD 22; (G) NIGP 174015; (H) NIGP 174016. (I, J) *Cordylodus intermedius* Furnish, 1938, lateral view; (I) compressed element, BD 23A, NIGP 23A002; (J) rounded element, BD 24, NIGP 174011. (K–M) *Cordylodus lindstromi* Druce

and Jones, 1971, lateral view; (K) compressed element, BD 30, NIGP 182033; (L) rounded element, BD 30, NIGP 182032; (M) rounded element, BD 28B, NIGP 182030. (N) *Utahconus beimadaoensis* Chui and Zhang in An et al., 1983, lateral view, BD 30A, NIGP 30A002. (O, P) *Iapetognathus jilinensis* Nicoll, Miller, Nowlan, Repetski and Ethington, 1999, left and right elements, upper view, BD 29, NIGP 173046 and NIGP 29002. (Q) *Cordylodus prion* Lindström, 1955, *sensu* Nicoll (1991), rounded element, outer lateral view, BD 19, NGIP 19001. Scale bars represent 200 um. All figured specimens are housed in Nanjing Institute of Geology and Palaeontology, Chinese Academy of Sciences, Nanjing, China (acronym: NIGP).

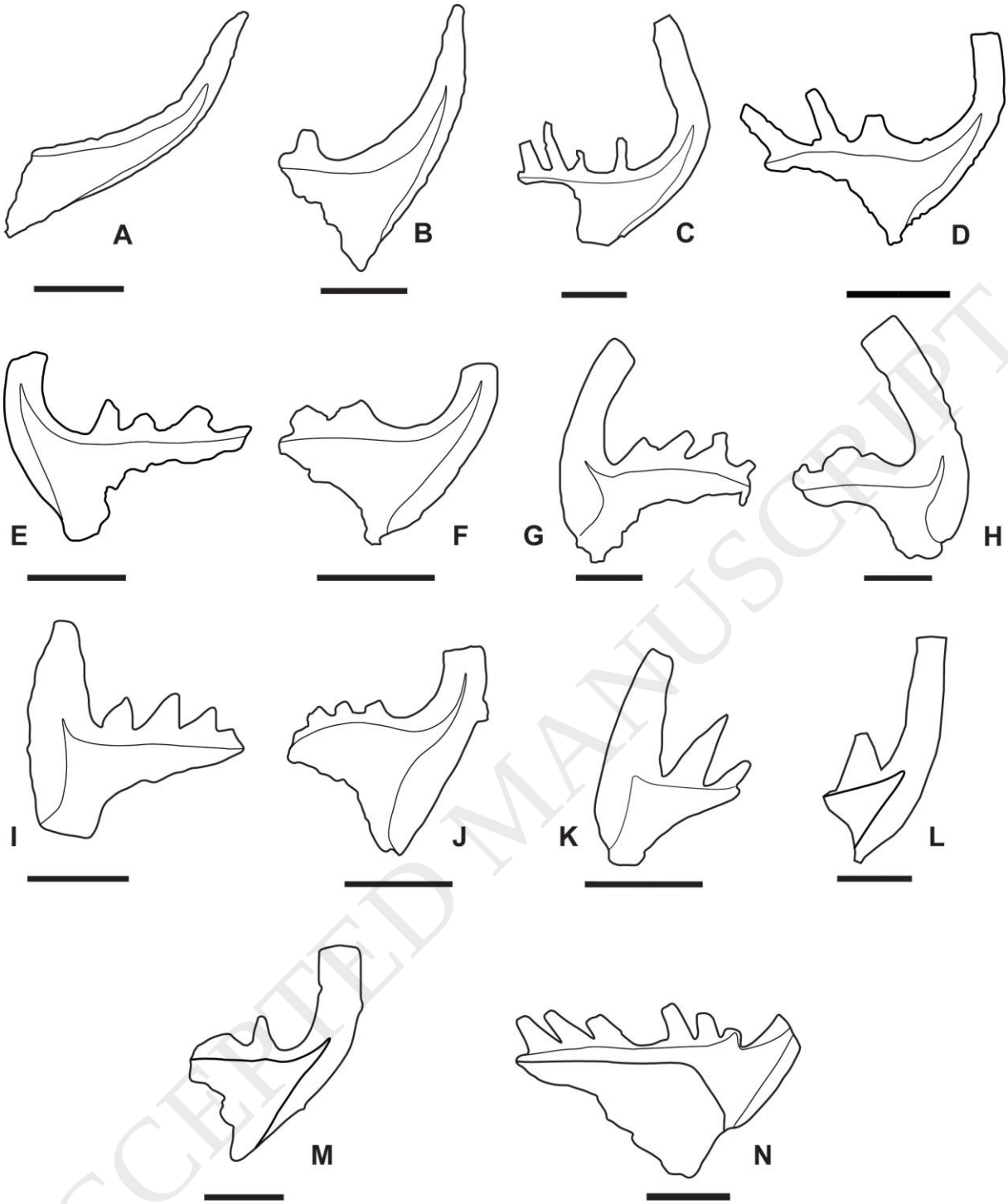

Fig. 5. Linedrawings of selected conodont species from Fig. 4 showing the outline of the basal cavity. (A) *Eoconodontus notchpeakensis*, Miller, 1969, lateral view, BD 15, NIGP 174030 (same specimen as Fig. 4A). (B) *Cordylodus primitivus* Bagnoli, Barnes and Stevens, 1987, lateral view, BD 15, NIGP 174044 (same specimen as Fig. 4B). (C, D) *Cordylodus proavus* Müller, 1959, rounded elements, lateral view, BD 8B, NIGP 8B001 and NIGP 174034 (same specimens as Fig. 4C, D). (E, F) *Cordylodus caboti* Bagnoli, Barnes and Stevens, 1987, rounded elements, lateral view; (E) BD 23A, NIGP 23A001; (F) BD 22, NIGP

174017 (same specimens as Fig. 4E, F). (G, H) *Cordylodus drucei* Miller, 1980, outer lateral view, BD 22; (G) NIGP 174015, (H) NIGP 174016 (same specimens as Fig. 4G, H). (I, J) *Cordylodus intermedius* Furnish, 1938, lateral view; (I) compressed element, BD 23A, NIGP 23A002; (J) rounded element, BD 24, NIGP 174011 (same specimens as Fig. 4I, J). (K–M) *Cordylodus lindstromi* Druce and Jones, 1971, lateral view; (K) compressed element, BD 30, NIGP 182033; (L) rounded element, BD 30, NIGP 182032; (M) rounded element, BD 28B, NIGP 182030 (same specimens as Fig. 4K–M). (N) *Cordylodus prion* Lindström, 1955, *sensu* Nicoll (1991), rounded element, outer lateral view, BD 19, NGIP 19001 (same specimen as Fig. 4Q). Scale bars represent 200 um.

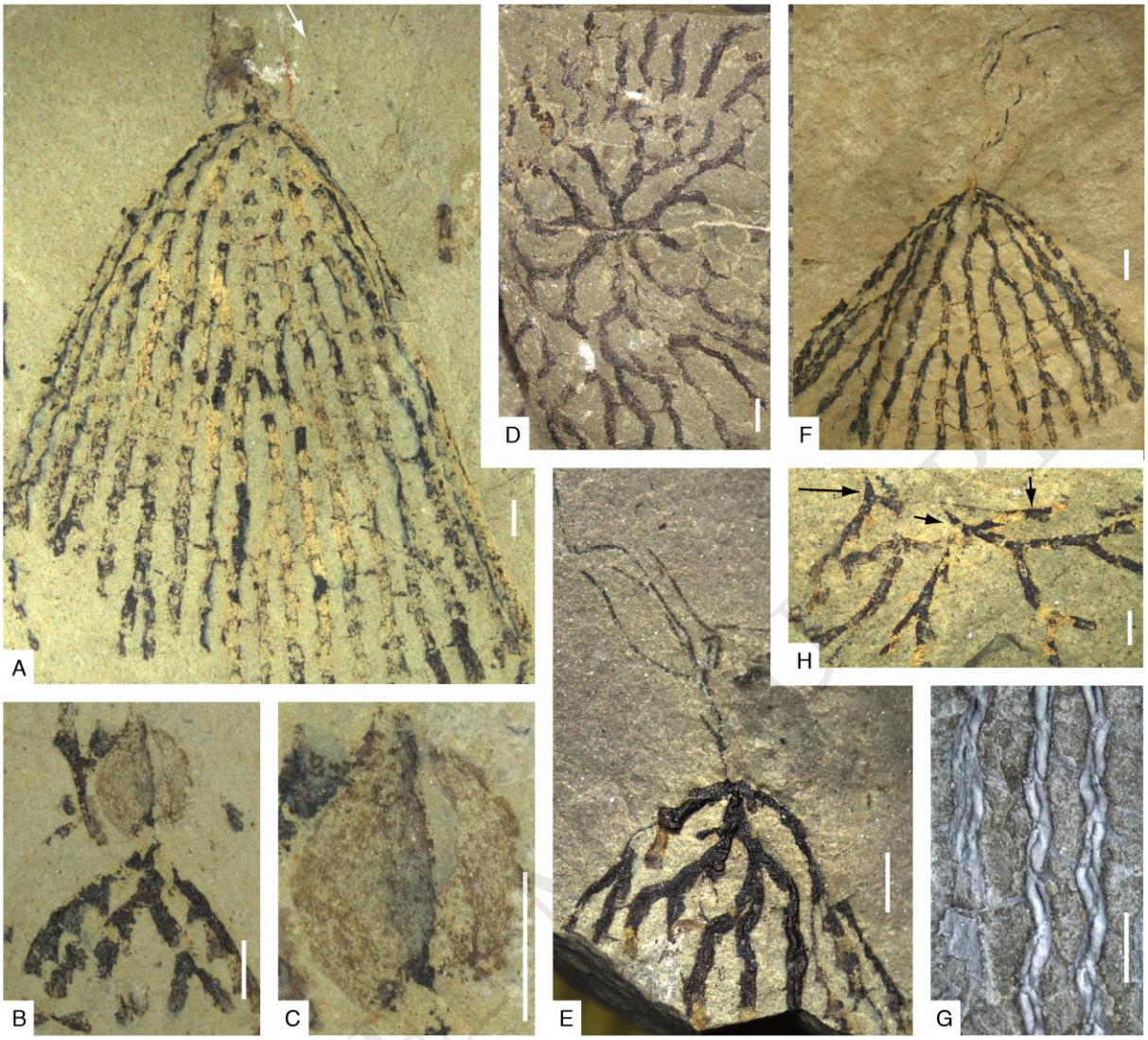

Fig. 6. (A–C) *Rhabdinopora proparabola* (Lin, 1986); (A) NIGP 98646, larger specimen with fragmented proximal structure showing colony shape; (B, C) NIGP 98605, small specimen showing three-vaned proximal structure, note fusellar construction in (C). (D–G) *Rhabdinopora parabola* (Bulman, 1954); (D) NIGP 168426, dorsal view showing quadriradiate development; (E, F) NIGP 168427 and NIGP 164496, laterally preserved specimens showing colony shape and branched nemata; (G) NIGP 168428, stipe fragment in relief, coated with ammonium chlorite. (H) *Anisograptus matanensis* Ruedemann, 1937, NIGP 168429, several small specimens showing sicula (arrows). Scale bars represent 1 mm. All figured specimens are housed in Nanjing Institute of Geology and Palaeontology, Chinese Academy of Sciences, Nanjing, China (acronym: NIGP).

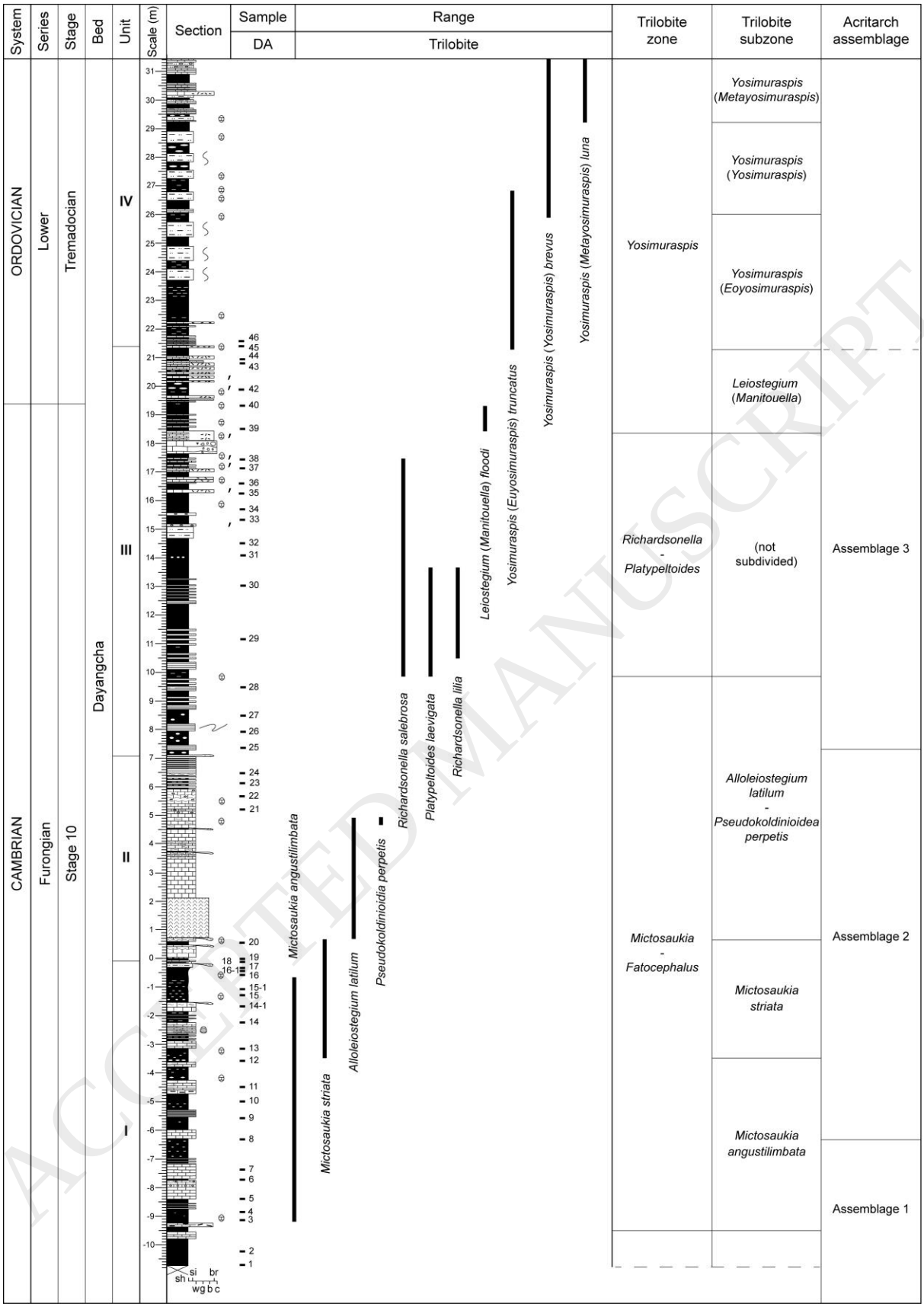

Fig. 7. Upper Cambrian to Lower Ordovician (Tremadocian) acritarch and trilobite biostratigraphy of the Xiaoyangqiao section. For legend, see Fig. 10. Abbreviations used for

grainsize: sh = shale; si = siltstone; br = breccia; w = wackestone; g = grainstone; b = boundstone; c = conglomerate.

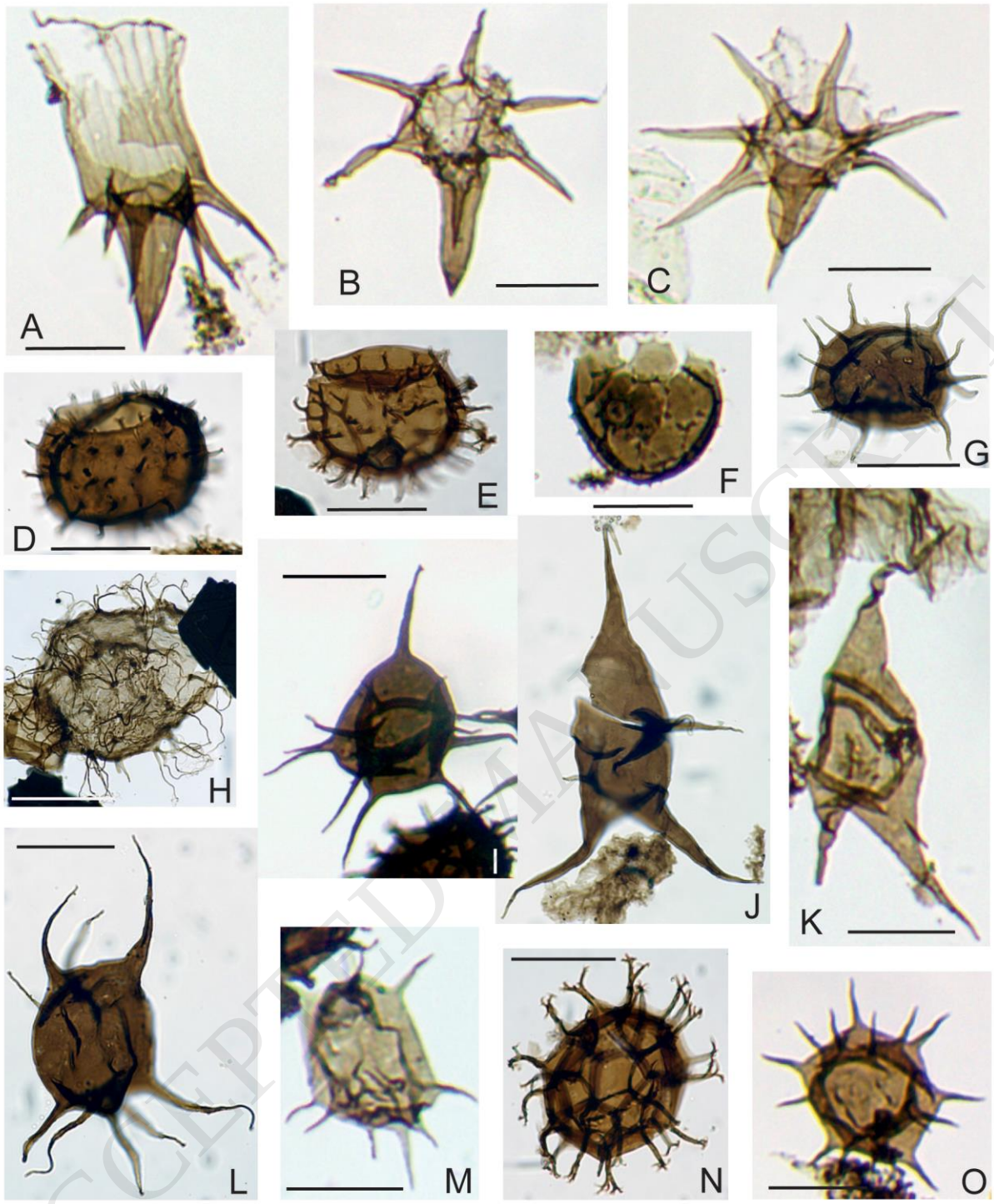

Fig. 8. Representative late Cambrian (Furongian) to Lower Ordovician acritarchs species from the Xiaoyangqiao section. The sample/slide number and England Finder coordinates are indicated for all specimens. (A–C) *Corollasphaeridium wilcoxianum* Martin in Martin and Dean, 1982; (A) specimen in lateral view, sample DA 36, E31/3; (B, C) specimens in compressed transverse view, sample DA 36, B51/1 (B), P55/1 (C). (D) *Stelliferidium stelligerum* (Gorka, 1967) Deunff et al., 1974, sample DA 15, T42/2. (E) *Cymatiogalea* aff. *C. bouvardii* Martin, 1973, sample DA 15, H27/1. (F) *Cymatiogalea cuvillieri* (Deunff, 1961)

Deunff, 1964, sample DA 37, V39/2. (G) *Actinotodissus achrasi* (Martin, 1983) Martin and Dean, 1988, sample DA 15, F31/1,3. (H) *Vulcanisphaera africana* (Deunff, 1961) Rasul, 1976, sample DA 15, L23/3,4. (I) *Ninadiacrodium caudatum* (Vanguestaine, 1973) Raevskaya and Servais, 2009, sample DA 15, C42. (J) *Ninadiacrodium* sp. A, sample DA 15, F29/2,4. (K) *Ninadiacrodium dumontii* (Vanguestaine, 1973) Raevskaya and Servais, 2009, sample DA 15, S51/3. (L, M) *Dasydiacrodium obsonum* Martin in Martin and Dean, 1988; (L) sample DA 15, L47/3; (M) sample DA 15-1, L46/2. (N) *Timofeevia phosphoritica* Vanguestaine, 1978, sample DA 4, H34/2. (O) Acritarch ex. gr. *Polygonium–Solisphaeridium*, sample DA 4, K48. Scale bars represent 20 µm.

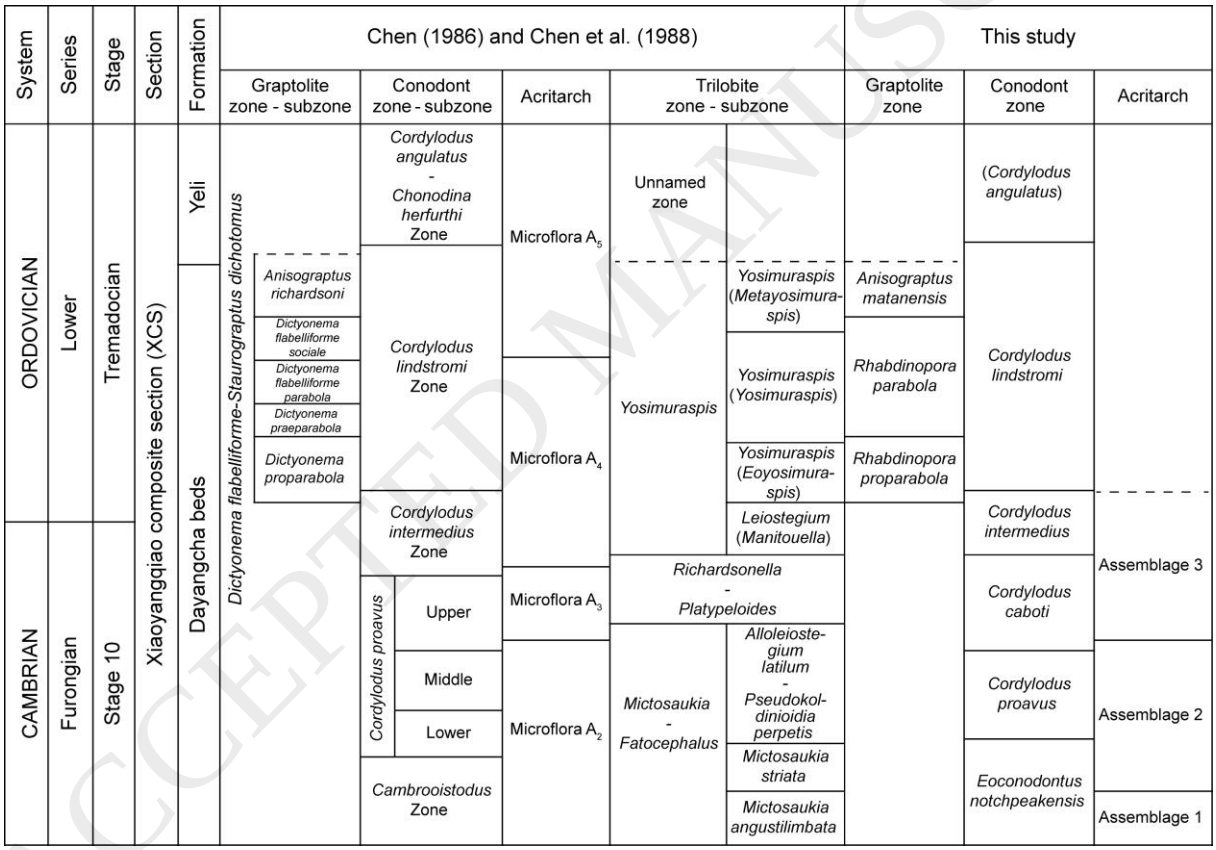

Fig. 9. Comparison between the integrated zonation systems of Chen (1986) and Chen et al. (1988) and this study. The trilobite zonation is the same for both studies.

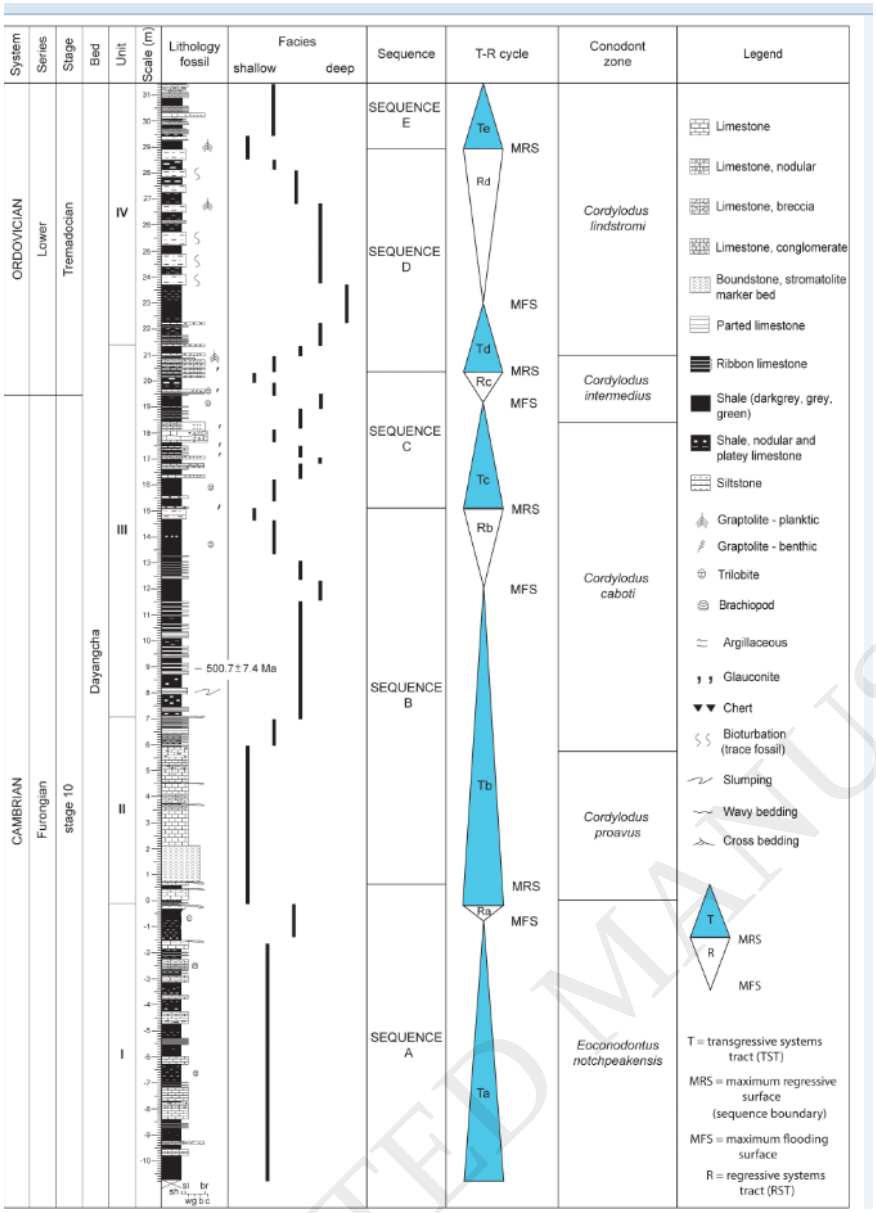

Fig. 10. T-R sequence stratigraphy of the Xiaoyangqiao section. The sequences are based on the T-R procedure promoted by Embry and Johannessen (1992). The sequences are of 3rd and higher order. Abbreviations used for grainsize: sh = shale; si = siltstone; br = breccia; w = wackestone; g = grainstone; b = boundstone; c = conglomerate.

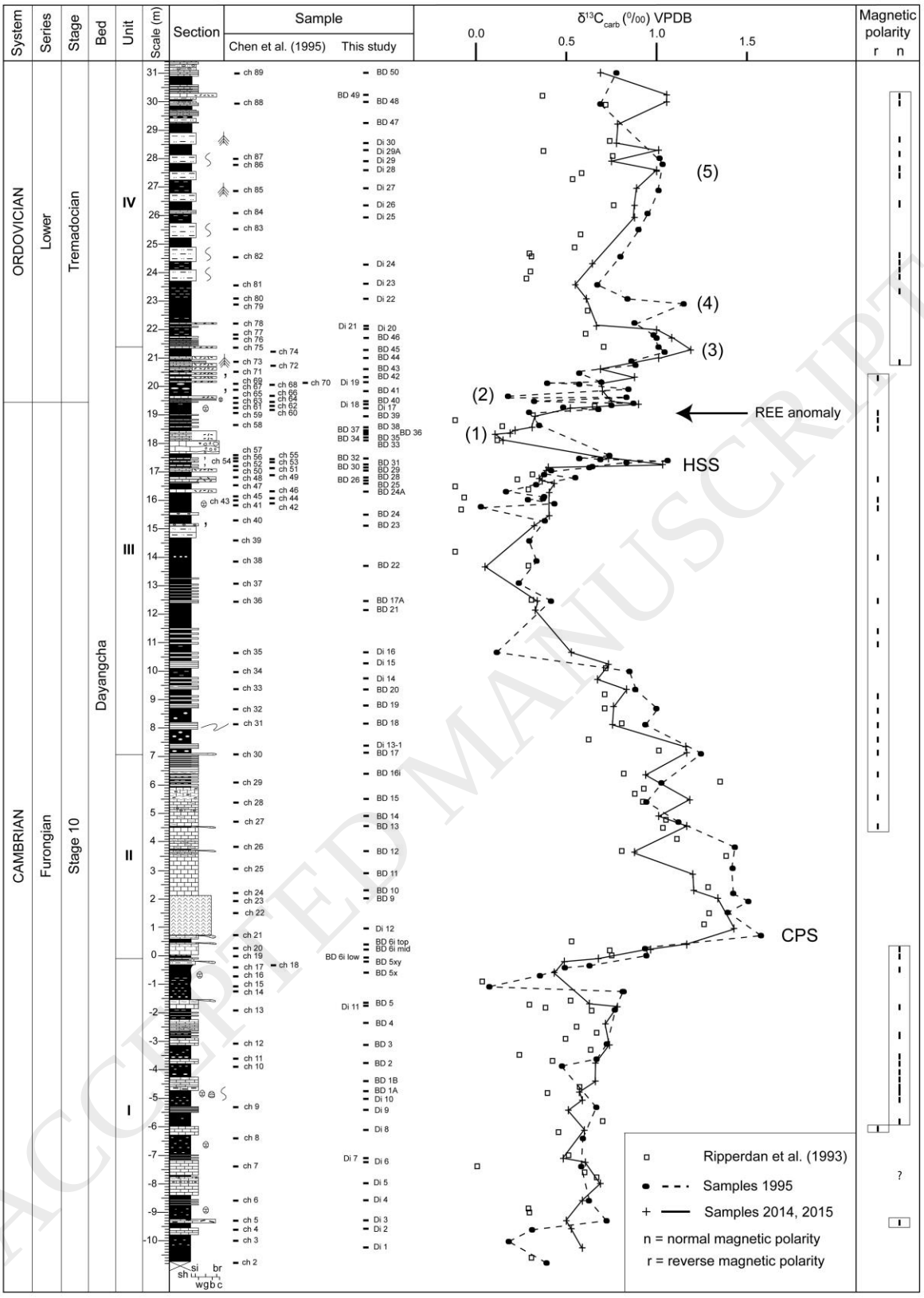

Fig. 11. C-isotope curves and magnetic polar reversals from the Xiaoyangqiao section. The C-isotope curves are respectively from Ripperdan et al. (1993; small squares), Chen et al. (1995; dots and dotted lines) and this study (+ and unbroken lines). The magnetic reversal data are

from Ripperdan et al. (1993) and Chen et al. (1995, table 2). For details see text. For Legend, see Fig. 10. Abbreviations used for grainsize: sh = shale; si = siltstone; br = breccia; w = wackestone; g = grainstone; b = boundstone; c = conglomerate.

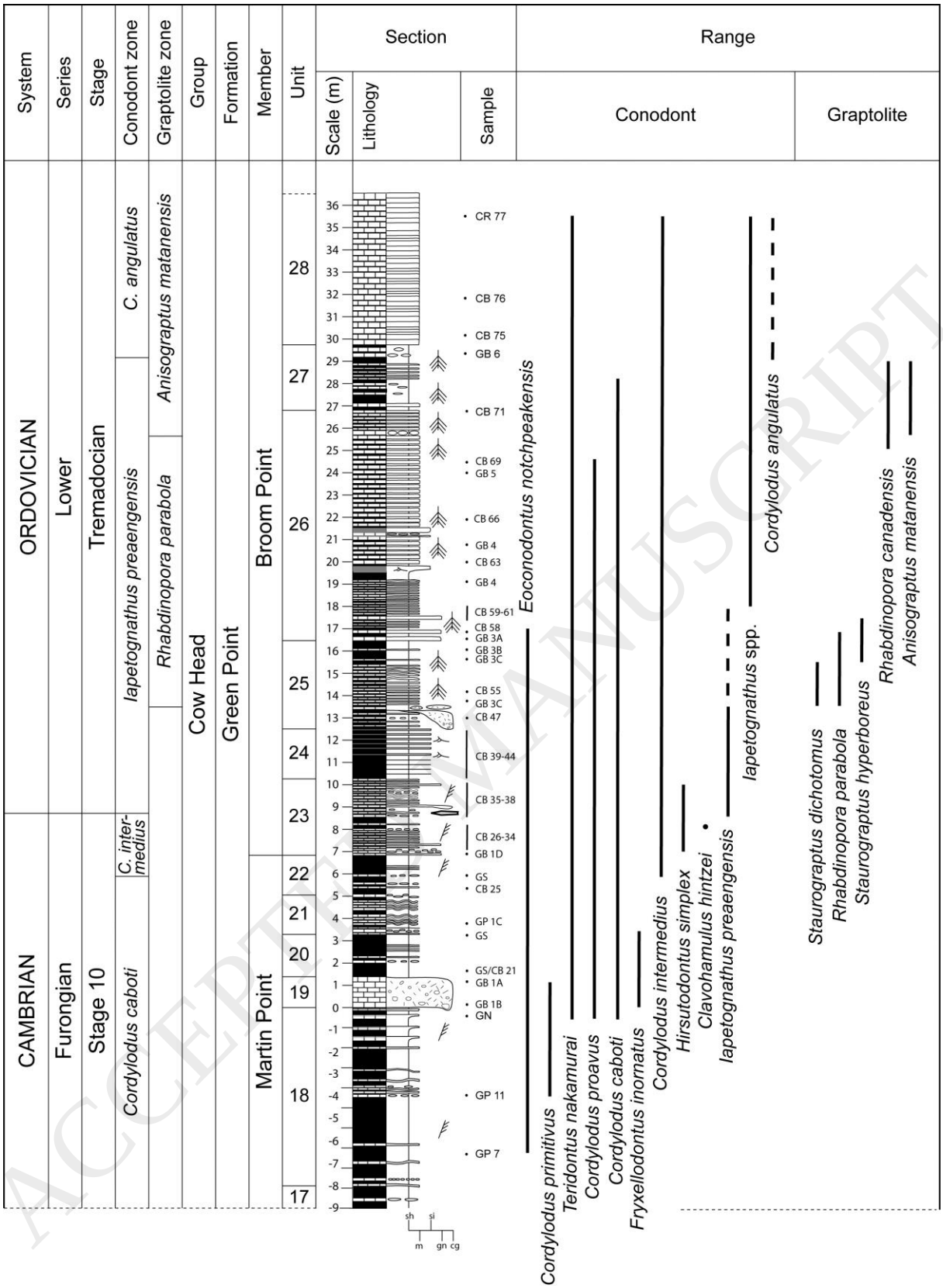

Fig. 12. Upper Cambrian to Lower Ordovician stratigraphy of the Green Point GSSP section with conodont and graptolite ranges and zones. The GSSP horizon is marked by a 'golden spike' in unit 23. The samples are from Barnes (1988, CB), (Bagnoli et al., 1987, GB) and

own collection (GS, GN). For legend, see Fig. 10. Abbreviations used for grainsize: sh = shale; si = siltstone; m = mudstone; gn = grainstone; cg = conglomerate.

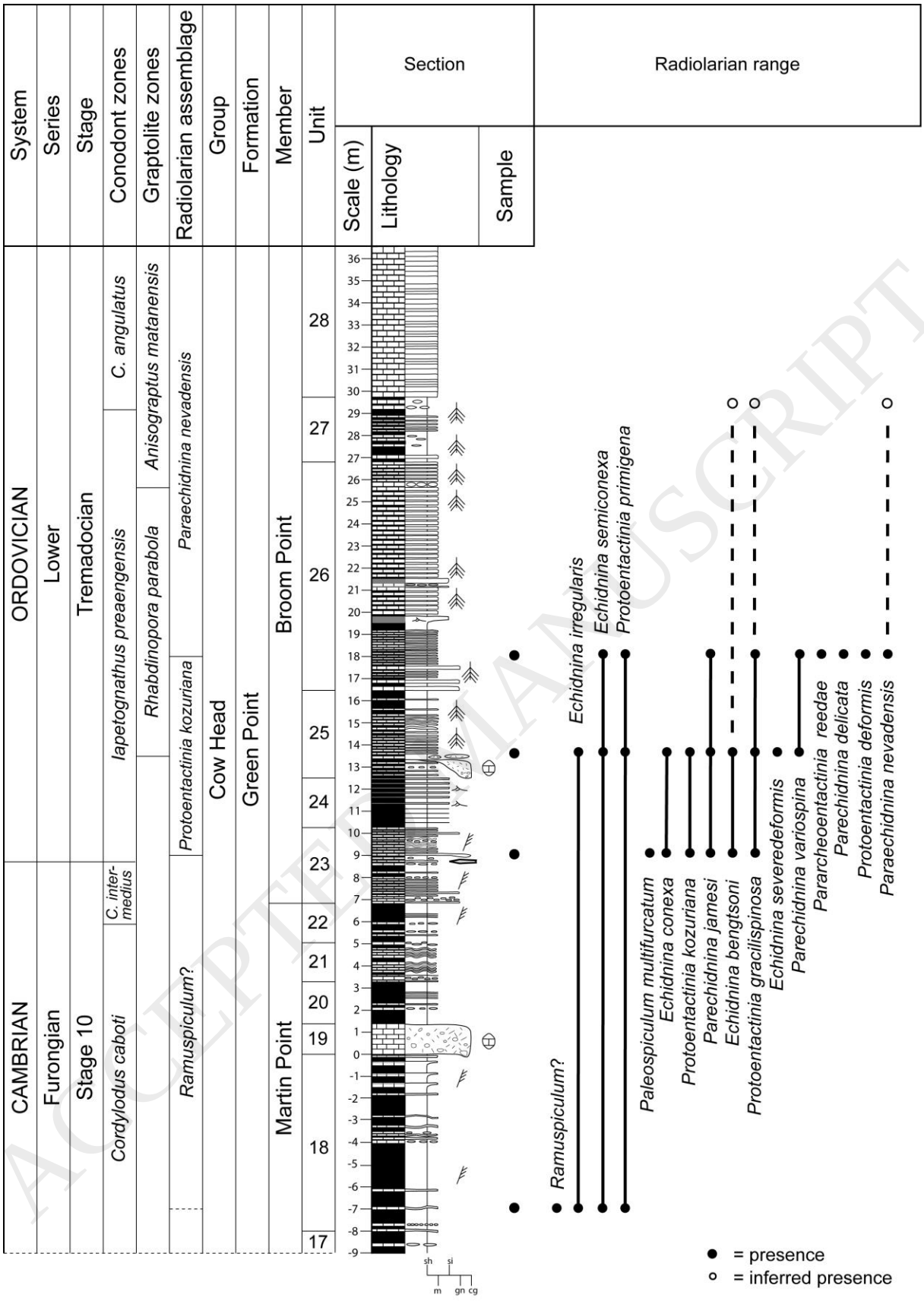

Fig. 13. Upper Cambrian to Lower Ordovician radiolarian biostratigraphy at Green Point (*Parechidina nevadensis* level of Kozur et al., 1996, *Cordylodus angulatus* conodont zone)

from Nevada is added. The *Ramuspiculum* assemblage(?) from unit 18 correlates with the *C. caboti* Zone. The *Protoentactinia kozuriana* and *Paraechidnina nevadensis* radiolarian assemblages correlate with the *Iapetognathus preaengenis* Zone and the *R. parabola* Zone. Species of the latter radiolarian assemblage extends into the *C. angulatus* Zone (Kozur et al., 1996) and the *Anisograptus matanensis* Zone. For legend, see Fig. 10. Abbreviations used for grainsize: sh = shale; si = siltstone; m = mudstone; gn = grainstone; cg = conglomerate.

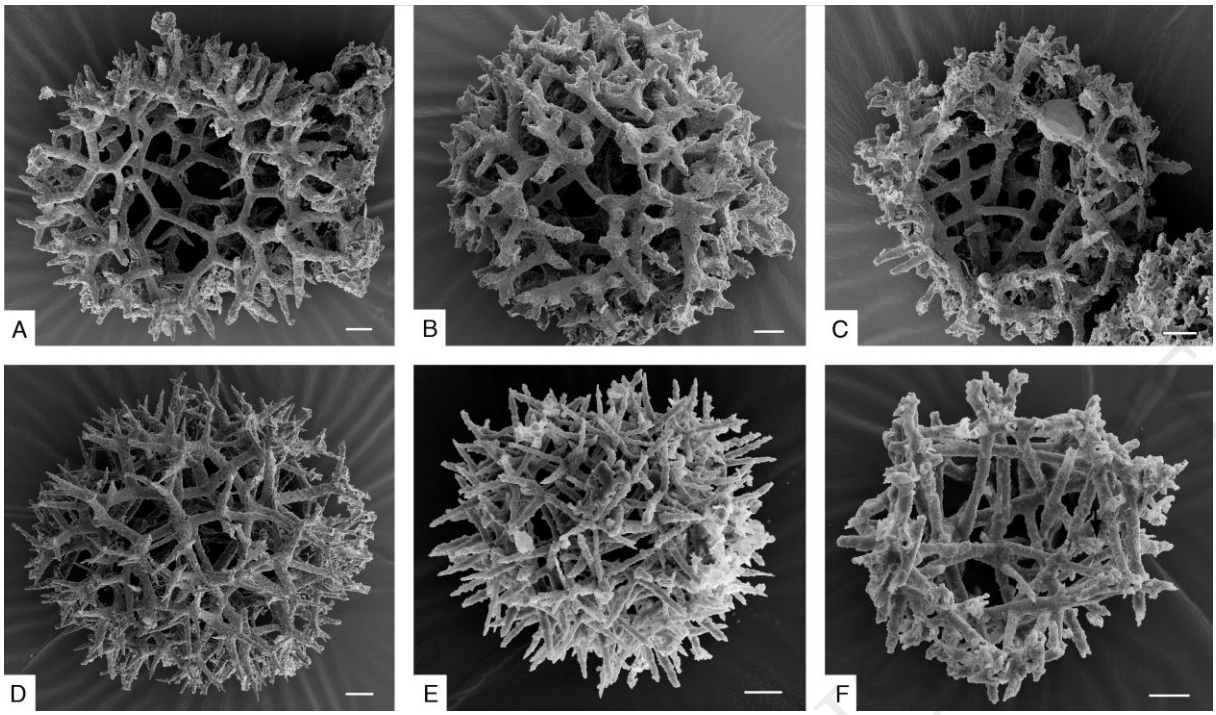

Fig. 14. Representative lowermost Ordovician radiolarian species from the *Protoentactinia kozuriana* assemblage, basal Tremadocian, Green Point GSSP section. (A, D) *Protoentactinia gracilispinosa*, GSC 140463 and GSC 140464. (B, C) *Protoentactinia kozuriana*, GSC 140465 and GSC 140466. (E, F) *Echidnina conexa*, GSC 140467 and GSC 139213 (*Subechidnina* sp. in Maletz, 2017, fig. 2.6). Scale bars represent 20 µm.

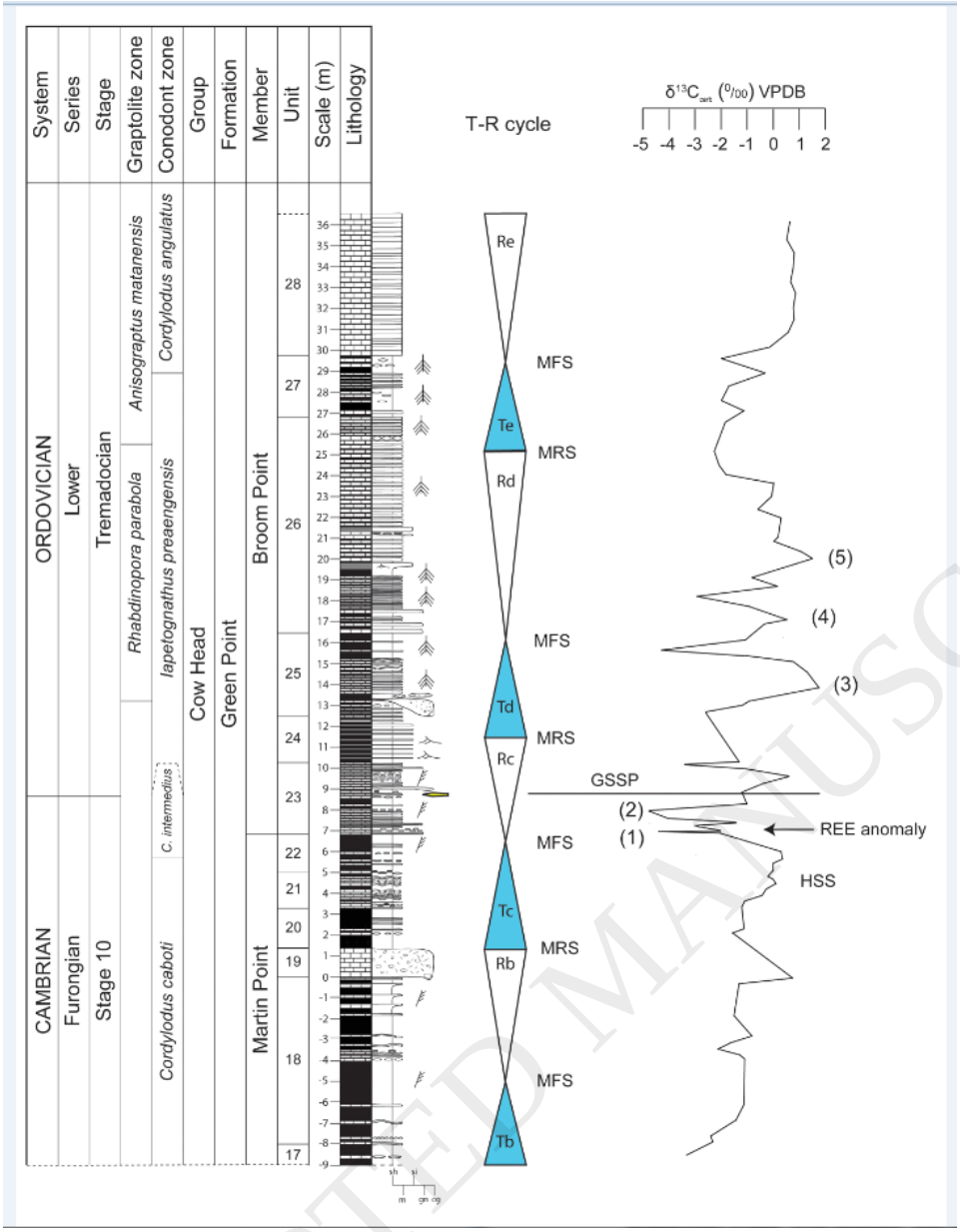

Fig. 15. Detailed sequence stratigraphy, C-isotope curve and geochemical anomaly of the Green Point GSSP Section. The numbered spikes are interpreted to represent the same spikes as for the Xiaoyangqiao section shown in Fig. 10. The GSSP horizon lies within the Regressive System Tract (Rc). The large C-isotope peak (3) coincides with the base of the *R. parabola* Zone in the Green Point section, (4) corresponds to the *Rhabdinopora parabola* Zone *sensu* Cooper et al. (2001), and the broad spike (5) marks the *Anisograptus matanensis* graptolite Zone. For legend, see Fig. 10. Abbreviations used for grainsize: sh = shale; si = siltstone; m = mudstone; gn = grainstone; cg = conglomerate.

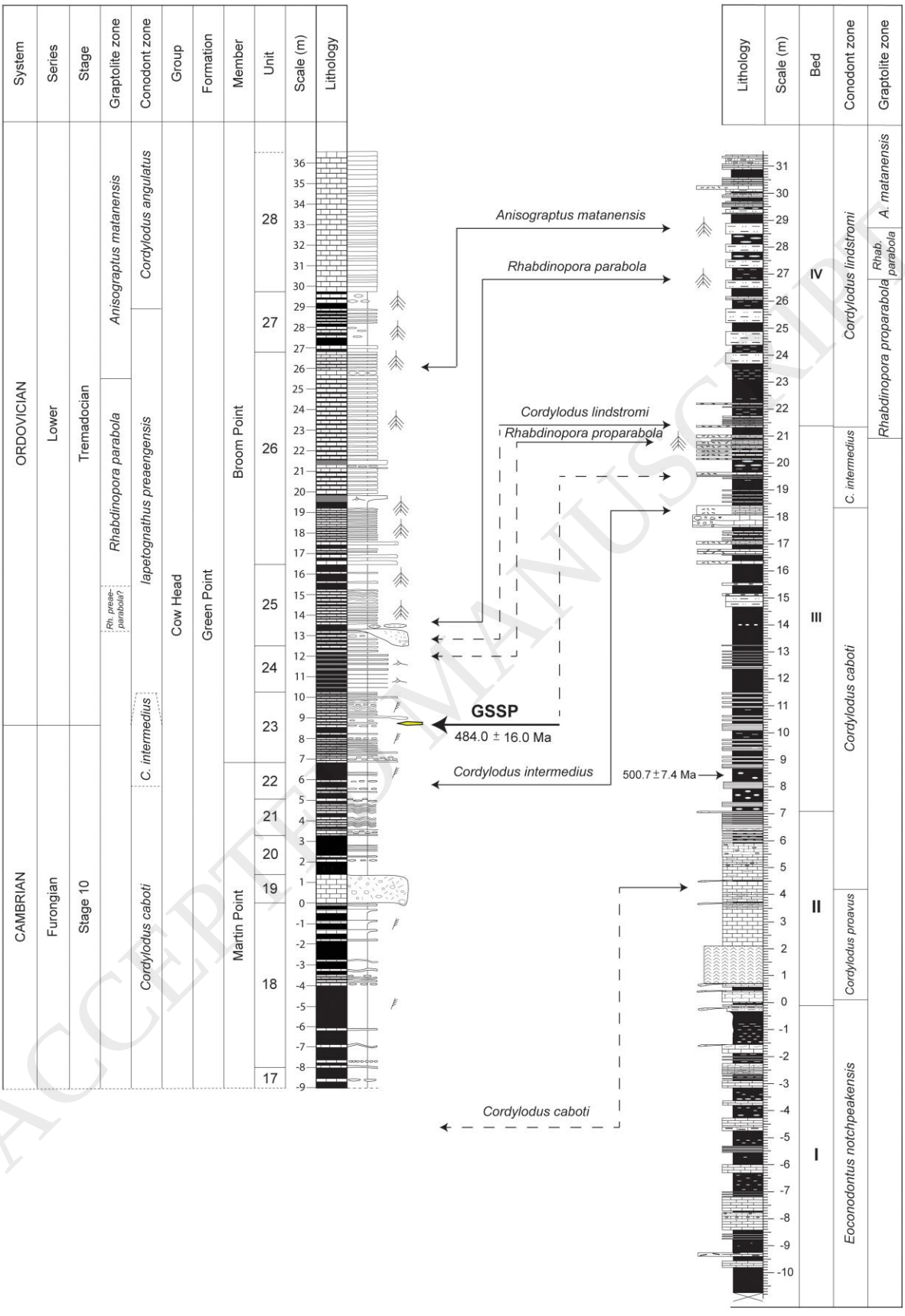

Fig. 16. Detailed biostratigraphic correlation of the Xiaoyangqiao section and the Green Point GSSP section. Unbroken lines and arrows point at direct evidence. The dashed lines represent the likely position and interpreted correlation of a taxon that is represented in only one of the sections. For legend, see Fig. 10 (for grainsize: see Figs. 12, 13 and 15).

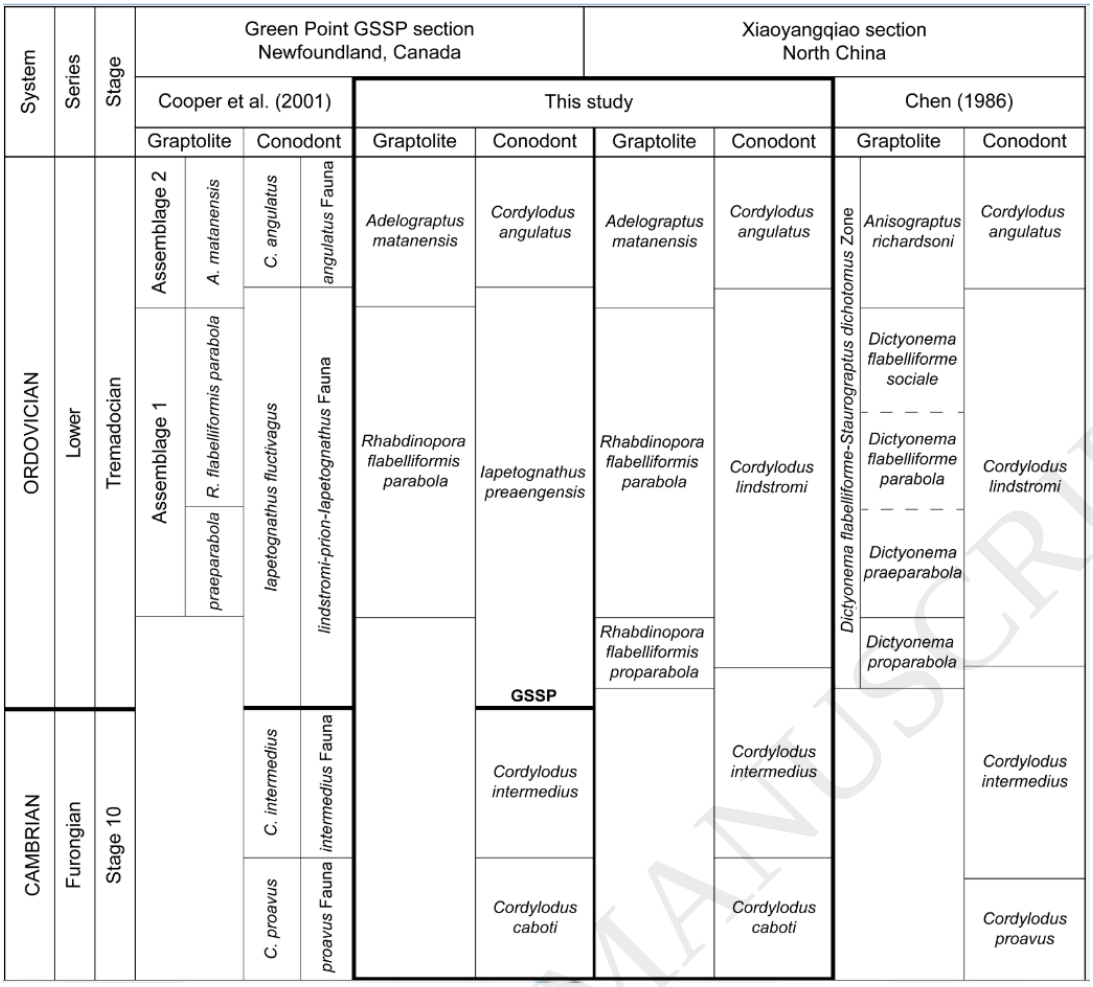

Fig. 17. Summary of the precise correlation and match of the Xiaoyangqiao section, North China and the Green Point GSSP section, western Newfoundland, Canada. The GSSP horizon lies within the upper *Cordylodus intermedius* conodont Zone and below the first appearance of planktic graptolites. The GSSP horizon is above the Lower House lowstand and below the 'Acerocare Regressive Event' in the Green Point succession.

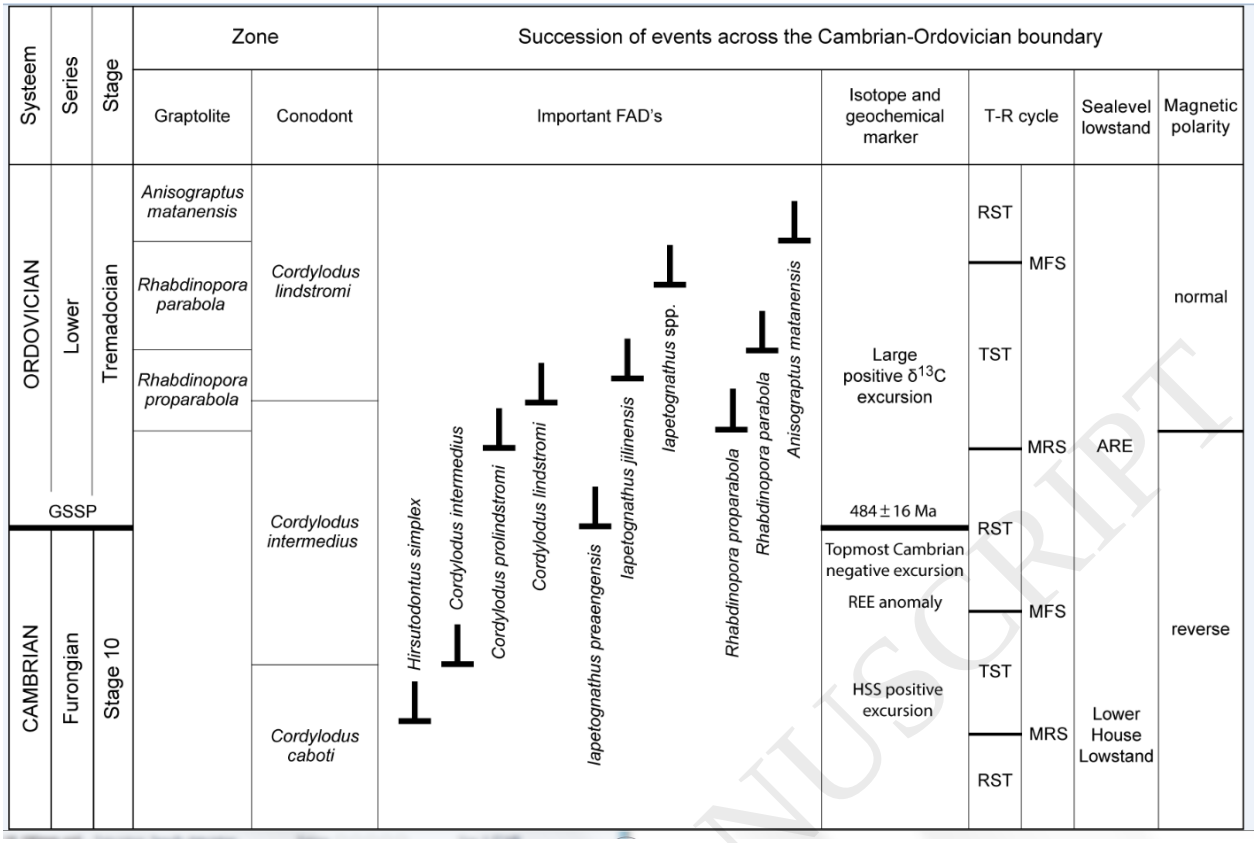

Fig. 18. Succession of events in the late Cambrian and earliest Ordovician. All events are useful as proxies for the recognition of the base of the global Ordovician System.